SAHC

Aging tests to assess the durability of building materials to salt crystallization - towards a more realistic and effective use of sodium sulfate

Krista MacWilliam

Czech Republic | 2017

ADVANCED MASTERS IN STRUCTURAL ANALYSIS
OF MONUMENTS AND HISTORICAL CONSTRUCTIONS

Master's Thesis

Krista MacWilliam

Aging tests to assess the durability of building materials to salt crystallization - towards a more realistic and effective use of sodium sulfate

Czech Technical University in Prague

UPC
UNIVERSITAT POLITÈCNICA DE CATALUNYA

Education and Culture

Erasmus Mundus

ADVANCED MASTERS IN STRUCTURAL ANALYSIS
OF MONUMENTS AND HISTORICAL CONSTRUCTIONS

Master's Thesis

Krista MacWilliam

Aging tests to assess the durability of building materials to salt crystallization - towards a more realistic and effective use of sodium sulfate

This Masters Course has been funded with support from the European Commission. This publication reflects the views only of the author, and the Commission cannot be held responsible for any use which may be made of the information contained therein.

Czech Republic | 2017

CZECH TECHNICAL UNIVERSITY IN PRAGUE
Faculty of Civil Engineering
Thákurova 7, 166 29 Prague 6, Czech Republic

MASTER'S THESIS PROPOSAL

study programme:	Civil Engineering
study branch:	Advanced Masters in Structural Analysis of Monuments and Historical Constructions
academic year:	2016/2017

Student's name and surname:	Krista MacWilliam
Department:	Department of Mechanics
Thesis supervisor:	Cristiana Nunes
Thesis title:	Aging tests to assess the durability of building materials to salt crystallization – towards a more realistic and effective use of sodium sulfate
Thesis title in English	see above

Framework content: The objective of this thesis was to work toward developing a more representative accelerated salt crystallization test for masonry construction materials. This was done through the investigation of various environmental and procedural factors that impact the efficacy and realistic nature of crystallization tests. The EN 12370 standard was used as the baseline and four variations were developed and performed. Comparison of the different testing conditions are discussed and recommendation on the most relevant conditions for future accelerated salt aging tests are given.

Assignment date: 7/04/2017 Submission date: 04/07/2017

If the student fails to submit the Master's thesis on time, they are obliged to justify this fact in advance in writing, if this request (submitted through the Student Registrar) is granted by the Dean, the Dean will assign the student a substitute date for holding the final graduation examination (2 attempts for FGE remain). If this fact is not appropriately excused or if the request is not granted by the Dean, the Dean will assign the student a date for retaking the final graduation examination, FGE can be retaken only once. (Study and Examination Code, Art 22, Par 3, 4.)

The student takes notice of the obligation of working out the Master's thesis on their own, without any outside help, except for consultation. The list of references, other sources and names of consultants must be included in the Master's thesis.

Laura Paulos k.
Master's thesis supervisor

Head of department

Date of Master's thesis proposal take over: July 2017

Krista MacWilliam
Student

This form must be completed in 3 copies – 1x department, 1x student, 1x Student Registrar (sent by department)

DECLARATION

Name:	Krista MacWilliam
Email:	krista.macwilliam@carleton.ca

Title of the Msc Dissertation:	Aging tests to assess the durability of building materials to salt crystallization – towards a more realistic and effective use of sodium sulfate
Supervisor(s):	Mgr.Cristiana Nunes, Ph.D.
Year:	2017

I hereby declare that all information in this document has been obtained and presented in accordance with academic rules and ethical conduct. I also declare that, as required by these rules and conduct, I have fully cited and referenced all material and results that are not original to this work.

I hereby declare that the MSc Consortium responsible for the Advanced Masters in Structural Analysis of Monuments and Historical Constructions is allowed to store and make available electronically the present MSc Dissertation.

University:	Czech Technical University in Prague
Date:	July 4, 2017
Signature:	

This page is left blank on purpose.

ACKNOWLEDGEMENTS

I would first like to thank my supervisor Mgr. Cristiana Nunes from the Institute of Theoretical and Applied Mechanics (ITAM). She was always available to answer questions and helped guide me in carrying out my thesis work. Without her enthusiasm and technical expertise, I would not have been able to make the most of the short time I had to complete my thesis.

I would also like to extend my appreciation to the numerous other individuals who work at ITAM who helped me during my time there. To the directors, professors Miloš Drdácký, PhD., DSc. and Stanislav Pospíšil, Ph.D., for receiving me at the Institute and facilitating my thesis research. Thank you to Pane Jan Válek Ph.D. for reviewing my thesis and aiding me in my experimental analysis. A big thank you to Mgr. Petra Hauková, Zuzana Slížková,Ph.D, and Dita Frankeová who helped me navigate the laboratory and acted as translators on countless occasions. To Pane Novák and Pane Slížkov for cutting and preparing all the test specimens I requested, regardless of how challenging the requirements were. Thank you to Ing. Jaroslav Valach, PhD. for his assistance in conducting the ultrasound testing and to Mgr. Veronika Koudelková for helping me perform and interpret the SEM analysis of numerous samples. Furthermore, thank you to everyone else at ITAM whom I met during my time working there. The people at ITAM always went out of their way to help me with my research and make me feel welcome; sometimes even in the face of large language barriers.

I would like to acknowledge the European Commission for the generous scholarship that aided me in being able to partake in this unique master's program. Thank you also to the Consortium and all the administrative people involved who facilitate this Masters program and ensure it runs smoothly. To the many professors from the partnering universities of the SAHC program (UPC, CTU, UMinho, and Unipd) thank you for sharing your vast expertise and enthusiasm for the field of heritage conservation throughout the duration of the Masters. In particular I would like to extend my appreciation to professors Pere Roca and Luca Pela at UPC and Professor Petr Kabele at CTU for managing the course work in Spain, and the dissertation work in the Czech Republic.

I am deeply gratefully to all of my family and friends back in Canada who supported me in my endeavor to do my Masters abroad. In particular to my mother, for the endless love and support. I cannot thank you enough.

Last, but certainly not least, I would like to thank all the other SAHC students who soldiered through this past year with me. Thank you for all the fun times and your enduring comradery through many a project. Thank you for sharing your knowledge, your passion, your cultures, your food, your wisdom, and your friendship with me. I am grateful to know I have made many more lifetime friends.

This page is left blank on purpose.

ABSTRACT

The damaging effect of salts in porous building materials is significant and widely spread, impacting structural and aesthetic aspects of historic constructions. To repair existing damage and mitigate future decay, a reliable testing procedure to quantify the durability of porous building materials to salt crystallization is needed. The objective of this thesis was to improve the ageing procedure of the most recent European standard (EN 12370) for assessing the durability of natural stone in respect to salt crystallization towards a more realistic and reliable way of reproducing the ageing conditions occurring in the field. This was done through the investigation of various environmental and procedural factors that impact the efficacy and realistic nature of salt crystallization. Existing knowledge and research in the field was studied to develop a state-of-the-art for identifying the main issues and develop strategies to overcome them. The EN 12370 standard was used as the baseline aging test. Four variations of the procedure were designed considering the effect of different testing conditions (salt solution concentration, temperature, contamination procedure). Experiments were carried out on three types of natural stone local to the Czech Republic and widely used in restoration interventions. The aim was to investigate the effect of the different ageing variables on the weathering of materials with different properties, namely regarding the porous structure and the mechanical strength. The ageing process was monitored using non-destructive techniques: visual observations and photographic documentation, salt solution uptake, mass variation and mass loss, and ultrasound pulse velocity. After the completion of the ageing tests, the specimens were also examined using destructive tests: salt distribution and microstructural analysis using scanning electron microscopy. Results of the different procedures showed the most difference in damage due to changes in the concentration of the salt solution. The contamination method and frequency also had significant, effect however it was also directly dependent on the nature of the porous network as well. Changes in drying temperature of the specimens had the least quantifiable impact on aging. A detailed comparison of the effect the different testing conditions had on the decay of the stones is discussed and recommendation on the most effective and realistic conditions for future accelerated salt aging tests are given.

Keywords: Salt Crystallization test, Durability, Sodium Sulfate, Building stone, Salt weathering simulation

This page is left blank on purpose.

ABSTRAKT

Posouzení odolnosti stavebních materiálů proti krystalizaci solí pomocí zkoušky stárnutí materiálu – praktické a efektivní použití síranu sodného

Škodlivý účinek solí v porézních stavebních materiálech patří mezi významné a široce rozšířené efekty, které ovlivňují strukturální a estetické aspekty historických staveb. Pro opravy stávajících poruch a zmírnění dalších poškození je zapotřebí stanovit spolehlivý zkušební postup k určení odolnosti stavebních materiálů proti krystalizaci solí. Cílem této práce je zdokonalit testovací postup nejnovější Evropské normy (EN 12370) prohodnocení odolnosti přírodního kamene ve vztahu ke krystalizací solí a upravit ho pro realističtější a spolehlivěji reprodukovatelný způsob stárnutí v terénu. To bylo provedeno zkoumáním různých environmentálních a procedurálních faktorů, které ovlivňují účinnost a reálný charakter krystalizace. V úvahu byly vzaty stávající znalosti a výzkum v této oblasti s cílem navrhnout nejvhodnější techniku k určení hlavních problémů a vypracovat strategie k jejich překonání. Norma EN 12370 byla použita jako základní test stárnutí materiálu, dále byly navrženy čtyři další varianty postupu s ohledem na různý vliv zkušebních podmínek (koncentrace solného roztoku, teplota, způsob kontaminace). Zkoušky byly provedeny na třech typech přírodního kamene z České republiky, které jsou běžně a široce používány při restaurátorských zásazích. Cílem bylo ověřit vliv různých proměnných faktorů stárnutí na zvětrávání materiálů s rozdílnými vlastnostmi, zejména pokud jde o porézní strukturu a mechanickou pevnost. Proces stárnutí byl kontrolován pomocí nedestruktivních technik: vizuálním pozorováním a fotografickou dokumentací, zaznamenáním absorpce solí, změny i ztráty hmotnosti a pomocí měření ultrazvukové pulzní rychlosti. Po dokončení testů stárnutí byly vzorky otestovány pomocí destruktivních metod: stanovení distribuce solí a mikrostrukturní analýzy za použití skenovací elektronové mikroskopie. Výsledky různých metod prokázaly největší rozdíly při poškození způsobeném změnami koncentrace solného roztoku. Metoda kontaminace a četnost měly také významný efekt, avšak ty byly i přímo závislé na povaze porézní sítě. Různá teplota sušení měla na stárnutí nejmenší stanovitelný dopad. Závěrem je diskutováno detailní srovnání rozdílných testovacích podmínek a jejich vliv na stárnutí kamene a doporučen postup pro dosažení realistických podmínek pro další zrychlené stárnutí pomocí solí.

Klíčová slova: Krystalizační zkouška, trvanlivost, síran sodný, stavební kámen, simulace solného zvětrávání.

This page is left blank on purpose.

TABLE OF CONTENTS

LIST OF FIGURES

LIST OF GRAPHS

LIST OF TABLES

1. INTRODUCTION

1.1 Motivation

It is well established that soluble salts are a major cause of damage to porous materials in the built environment. For a long time, salt's damaging effects have been seen in masonry buildings in varying degrees of severity. Soluble salts can cause aesthetic, moisture, material, and structural damage which are all inter related [1]. As many historic buildings are masonry structures, which are made of highly porous materials, the damage salt causes can be significant.

Currently, the main sources of salt include air pollutants (i.e: SO_x, NO_x, marine spray), salt-contaminated ground water (rising damp), as well as the building materials themselves (contaminated materials, i.e. poorly washed sand used in mortars, or through chemical reactions due to weathering agents involving moisture transport, i.e. leaching of sulphate products). Sodium sulfate (Na_2SO_4) specifically, occurs naturally and is produced as by-product to many manufacturing processes [2]. It is also reported as one of the most damaging salts found in deteriorated building materials [3] [4] [5].

Salt action can compromise the structural stability and the aesthetic aspect of heritage buildings. Therefore, it is essential to be able to assess the durability and compatibility of repair materials, with respect to salt crystallization, when planning a restoration intervention. This will enable selection of the most suitable repair materials, thus ensuring compatible preventive maintenance and restoration work can be carried out on historic structures and monuments. However, to achieve this, a standardized, realistic, and widely accepted testing protocol is required to ensure meaningful and consistent results. Presently the EN12370 standard for testing natural stone's durability to salt crystallization is often used, but also criticized for being excessively aggressive and unrealistic in simulating wreathing on-site. The complexity of understanding the behaviour of different salts and the characteristics of various porous building materials, compounded by trying to accurately represent real environmental conditions in the laboratory, all contribute to the present lack of representative and comprehensive testing.

1.2 Objectives

The objective of this research is to consider the existing tests used to determine the durability of stones under salt attack, develop potential alternative testing procedures, and assess their effectiveness. The focus of the aging tests performed is to improve the testing conditions prescribed in EN12370 to develop a more realistic accelerated procedure. As this is a very large and complex topic, the goal will be to consider the impact of sodium sulfate specifically. The scope of this dissertation was modeled on a portion of the scope of the recently created RILEM Technical Committee entitled "Accelerated laboratory test for the assessment of the durability of materials with respect to salt crystallization".

1.3 Thesis Outline

This thesis considers the existing body of knowledge on the subject of accelerated durability testing due to salt crystallization through a review of literature and standards. The theory and history of tests dealing

with salt crystallization are discussed. Furthermore, the physiochemical properties of sodium sulfate and characteristics of porous building materials are discussed in detail to understand how and why damage is caused.

Next, the methodology of the different tests and experiments conducted throughout the research is detailed. Following this, a section is dedicated to characterizing the three types of stone that were studied in this thesis. Available information on the porosity, pore size distribution (PSD), mechanical strength, petrography, and several other intrinsic characteristics that influence the durability of natural stone are presented.

The development of the new testing procedures considered is discussed. Modifications to the environmental and procedural factors of the EN12370 protocol, including the salt concentration, contamination conditions, frequency of recontamination, and drying temperature are elaborated. Following, the methodology for the testing techniques employed to analyse the results of the aging test are discussed. These techniques include visual observation, monitoring of mass evolution and mass loss, ultrasonic pulse velocity (UPV), microstructural analysis using scanning electron microscope (SEM), and evaluation of the salt distribution using electric conductivity measurements.

The results of all four variations of the EN12370 protocol are presented and compared in relation to the standard. Trends and anomalies observed through the various analysis methods are discussed in detail to develop a comprehensive and cohesive understanding of the impact each modified variable of the EN12370 standard has on the test results. Finally, in reference to the observed results, recommendations on the parameters that should be modified to help ensure a more realistic accelerated salt crystallization aging test procedure are given.

2. STATE OF THE ART

2.1 Existing Accelerated Aging Tests on Salt Crystallization

Deterioration due to cycles of salt crystallization-dissolution is a major cause of damage in historical building materials [6]. Salt weathering is a naturally occurring phenomenon due to the presence of salts and fluctuations in moisture and temperature. As previously mentioned, sources of salt contaminates include the construction material itself, interactions with atmospheric pollutants, ground water absorption, and even living microbes on the materials [6] [7] [8] [9]. The effects of salt attack can have significant aesthetic and physical ramifications. An example of its impact on the structure and decorative material the church of Sant Pere de Rubí in Spain, are shown in Figure 1. Due to these negative effects, assessing the durability of masonry materials to the impacts of salt crystallization is important for the conservation and restoration of historic monuments and buildings.

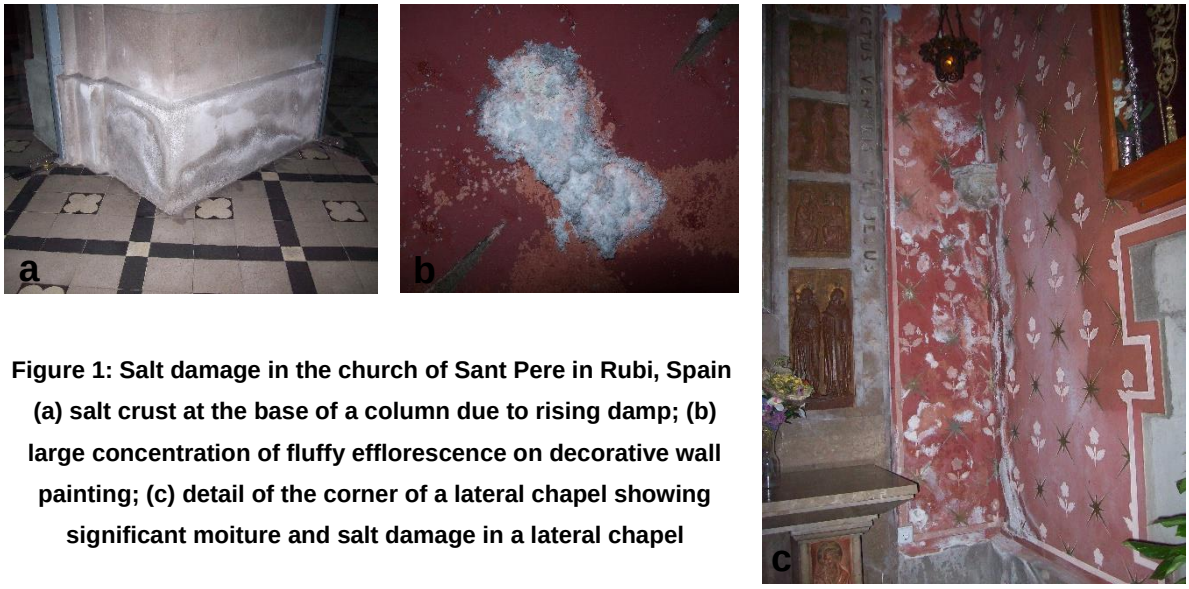

Figure 1: Salt damage in the church of Sant Pere in Rubi, Spain (a) salt crust at the base of a column due to rising damp; (b) large concentration of fluffy efflorescence on decorative wall painting; (c) detail of the corner of a lateral chapel showing significant moiture and salt damage in a lateral chapel

Assessing durability is not a new endeavour. Although the techniques used today may vary from those of the past, attempts to evaluate the durability of building materials have been documented for at least two thousand years. Prǐkryl [10] summarizes historic accounts of durability testing such as leaving stones outdoors in extreme weathering conditions (e.g. stacking blocks of stone in a beach) to weather for one to two years prior to selecting which stones to use. The first accelerated ageing testing recorded in 1828 aimed at assessing the resistance of stone to freeze-thaw cycles, but it used sodium sulfate as the ‘crystallization agent’ [10] [3].

Currently, several recommendations and standards exist to assess the durability of stones affected by salt crystallization (RILEM 1980, EN12370, WTA 2005, RILEM 1998). Attempts have also been made to develop mathematical models to predict the durability of masonry materials based on properties such as mechanical strength, crystallization pressure (i.e. pore size and supersaturation), salt transport during drying, and other factors [3]. However, some of these approaches do not transfer well into describing

the damage being seen on a micro and macro scale and the overall complexity of the problem has limited the validity of these models.

Laboratory testing also has its drawbacks, largely due to the difficulty in accurately simulating in-situ conditions in an experiment and accelerating the deterioration in a realistic approach. A detailed comparison of four of the most common tests currently used in the laboratory was done by Lubelli et al. [3]. The authors highlight that the aim of a reliable salt crystallization test is to assess and, if possible, predict the durability of a material (or materials) when used in a real construction.

Common laboratory accelerated salt crystallization procedures (RILEM 1980 V.1a, V.1b, and V.2, EN12370) involve cycles of combined contamination and wetting of the test specimen followed by drying in an oven for ≥15 hours. Contamination exposure is usually achieved through partial or complete immersion in a salt solution. Drying may be carried out at more moderate conditions as well, such as at a temperature of 20˚C and a relative humidity (RH) of 50% prescribed in RILEM (1998) MS-A.2. Alternative testing formats to the wet/dry cycles include humidity cycling [11] or continuous partial immersion (WTA 2005, RILEM 1998 MS-A.1). In any test, the most important factor to ensure is the occurrence of wet/dry cycles as this is the trigger for damage [3].

Different factors and conditions can greatly impact the results of the tests. To develop a realistic and reliable testing procedure, the question that needs to be answered is: which type of specimen (single or combined), salt type and concentration, contamination method, environmental factors (wet-dry cycles, continuous salt solution supply) and drying procedure will achieve realistic and reliable results?

Firstly, considering the type of specimen to be used, either single materials or combinations, such as masonry units or plaster-substrate systems, must be considered. The difference in the physical and chemical composition between two types of materials tested by themselves can change the behaviour and results of the test. Add in the interaction between a mortar and masonry unit with respect to physical aspects, chemical reactivity, and water transport mechanics, the situation becomes increasingly complex when considering all types of building assemblies that could be tested.

Salt type and load are other important factors since the type of salt changes how and when damaging stresses are developed, and concentration affects the quantity and rate of damage. For example, sodium sulfate (Na_2SO_4) and sodium chloride (NaCl) are reference salts widely used in durability tests. Due to their thermodynamic properties and kinetics of crystallization, sodium sulfate induces damage when thenardite is hydrated to mirabilite with liquid water, while sodium chloride causes damage during drying [3]. Additionally, to induce deterioration, enough salt must be present in the material to develop crystallization pressures greater than the mechanical strength of the material [9]. Contamination of specimens with low salt concentrations may take many crystallization-dissolution cycles to cause decay, while a high salt load may accelerate this process requiring less cycles for deterioration. However, high salt content can also slow the drying time of a specimen, requiring more time for each wet/dry cycle. In accelerated testing, the salt type should be selected to match the environment for which the material

will be used in. Additionally, some researchers recommend salt loads as low as 1-2%wt. for Na_2SO_4 and 2-4%wt. for NaCl [3].

An important way in which the contamination method can affect the results of an aging test is through the degree of saturation with salt solution. This factor is also largely dictated by the absorptive properties of the material. If partial immersion is employed, highly absorptive materials are likely to become saturated in a short period, whereas in the case of less absorptive materials, long periods may be required to reach saturation. Additionally, partial immersion allows absorption and evaporation to occur simultaneously, changing the dynamics of the water/salt solution transport mechanisms compared to complete immersion. Complete immersion ensures a more uniform salt distribution within the material. Immersion tests have been found to induce more damage, but they may not represent realistic in-situ conditions [5].

Environmental test conditions such as relative humidity, temperature, and air flow are significant both in the drying [3] and wetting phase [12]. Using more realistic environmental conditions can help to ensure that the damage mechanics reflect those occurring in natural exposure conditions. However, tests may take over a year to attain results [13]. In terms of drying time, increasing the temperature can accelerate this process, however this may negatively impact test results if the porous building material contains compounds whose structures change at elevated temperatures [3].

The methods of monitoring and evaluation of the deterioration mechanisms are a crucial aspect of any accelerated aging test. Monitoring through visual observation is the simplest approach, and some durability ratings such as the Alteration Index [4] rely on it. However, the subjectivity inherent to this approach can make comparing results between experiments impossible. Tracking the mass evolution is recurrently employed, as also prescribed in the EN12370 standard. Nevertheless, due to the competition between salt uptake and mass loss, interpreting changes in mass can be difficult. Other techniques used include evaluating the mechanical strength properties (e.g. dynamic modulus of elasticity), analysing microstructural alterations (e.g. with scanning electron microscopy (SEM), and assessing changes to the porous structure (e.g. using mercury intrusion porosimetry (MIP) [3] [5]. The challenge with a lot of these evaluation techniques is the influence the salt has on the results. Samples could be desalinated to determine the actual mass of only the test materials, or the alterations to the porous network for example, however this disrupts the aging process. Therefore, desalination and subsequent analytical testing is usually only completed at the end [3].

The impact and limitations of using different experimental conditions, in addition to the effects of the type of specimen, the salt type and concentration, additional environmental conditions, and the methods of assessment have on testing are all discussed in more detail by Lubelli et al. in [3]. Despite the several limitations outlined, laboratory accelerated salt crystallization tests are the most technically accessible approach for rating the resistance of porous building materials to salt damage.

2.2 Characteristics of Sodium Sulphate & Porous Building Materials

2.2.1 Sodium Sulfate phase diagram, thermodynamics, and kinetics of crystallization

It is well established that sodium sulfate (Na_2SO_4) is one of the most destructive salts for porous building materials [3] [4] [5]. The harmfulness of sodium sulfate is mainly due to in its tendency to supersaturate due to the differing solubility values of it's hydrated forms, which leads to high crystallization pressures [3]. Therefore, understanding sodium sulfate's potential for damage first requires an understanding of its intrinsic properties under varying environmental conditions, and then, how it interacts with porous building materials.

Depending on the temperature, and relative humidity of the environment, and the concentration of the solution, sodium sulfate can exist in several forms. In total, the salt can manifest in one of eight crystalline phases, however only five are seen at atmospheric pressure and within the temperature range considered for this research (≤110˚C) [7]. Of the five possible phases three are anhydrous states (phases III, IV, and V) and two are hydrates (hepta- and deca- hydrate). Of these, phase V (thenardite) and the decahydrate (mirabilite) are the stable forms while the other three are metastable [7] [8]. Therefore, the most likely phases to form are either the anhydrous thenardite (Na_2SO_4 (V)) or the decahydrate mirabilite ($Na_2SO_4 \cdot 10H_2O$) [7] [8], although the heptahydrate ($Na_2SO_4 \cdot 7H_2O$) has also been observed and studied in the lab and in-situ [14]. The various states and when they are formed are shown in the phase diagrams in Figure 2, which has been constructed with detailed and up-to-date theoretical and experimental data [8]. Relating to porous materials, the consensus in the field is that salts growing under supersaturation conditions and in confined spaces, like pores, will exert tensile stress on the material. As mentioned in [7] these forces can cause damage for masonry materials that generally have low tensile strengths, although Steiger and Asmussen address the issues of the macroscopic scale of tensile strength versus the microscopic scale of crystallization pressure and how a simple comparison

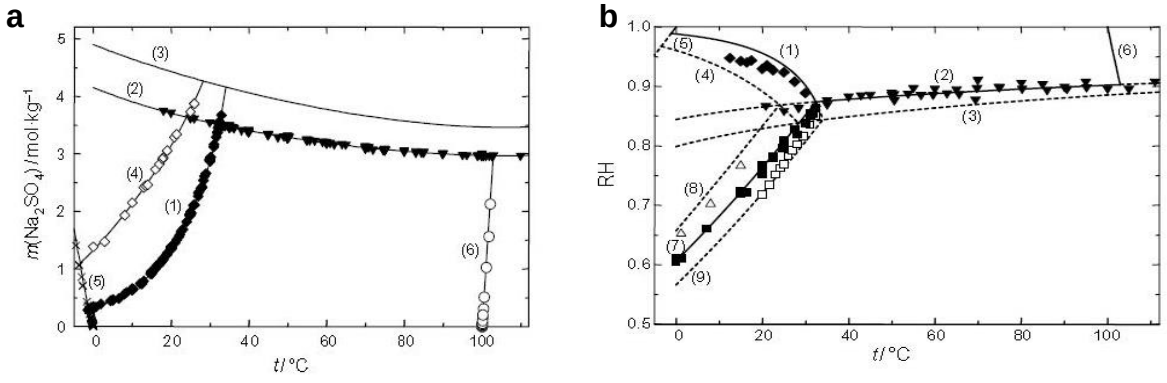

Figure 2 : Sodium sulfate phase diagrams constructed from theoretical and experimental data [4]

a) Phase diagram for variations in concentration and temperature: solubility of (1) $Na_2SO_4 \cdot 10H_2O$, (2) Na_2SO_4(V), (3) Na_2SO_4(III), (4) $Na_2SO_4 \cdot 7H_2O$, freezing temperatures (5), and boiling temperatures (6).
b) Phase diagram for variation in relative humidity and temperature. Curves represent stable (—) and metastable (---) equilibria; solid-solution equilibria (1)-(5) and the solution-vapour equilibrium (6) corresponds to the curves in (a) of this figure, the remaining curves represent solid-solid equilibria, i.e. (7) Na_2SO_4(V) - $Na_2SO_4 \cdot 10H_2O$, (8) Na_2SO_4(V) - $Na_2SO_4 \cdot 7H_2O$, and (9) Na_2SO_4(III) - $Na_2SO_4 \cdot 10H_2O$.

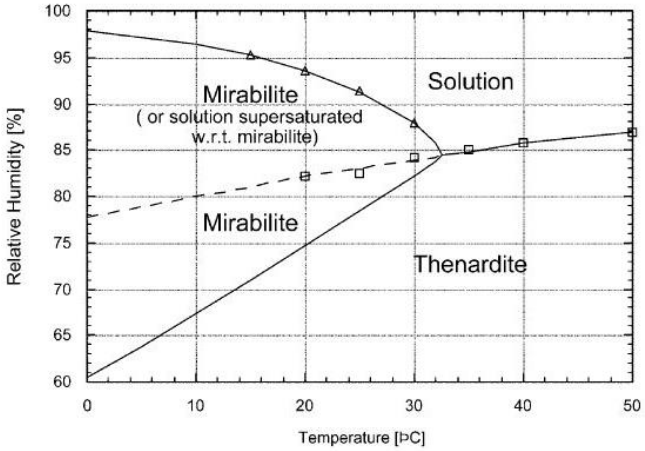

Figure 3: Simplified T-RH phase diagram of sodium sulfate [14]. The continuous lines indicate the boundaries of stable phases; discontinuous line corresponds metastable equilibrium.

of values isn't accurate to predict decay [8]. They state that two additional conditions must be met for damage to occur: firstly, a large portion of the pore wall must be in contact with the growing salt crystal, and second the stress from this crystal must be sufficiently large to propagate existing material flaws. Of the phases discussed, it is mirabilite that demonstrates the greatest ability to develop the required stresses to cause damage as its crystal structure occupies the greatest space, being 314% larger than thenardite crystals [7] [15] [5].

Solubility (Figure 2a) also significantly impacts the phase of sodium sulfate and is similarly dependent on temperature changes. Depicted in Figure 2a, the solubility curve of mirabilite (1) slopes upwards rapidly to the limit for stable mirabilite at temperature (T) of 32.4˚C [15] [5]; above which, mirabilite is theoretically in solution regardless of the concentration. In contrast, the solubility of thenardite changes very little with temperature and even decreases slightly with increasing temperature. However, the most important aspect is the relative solubility of thenardite and mirabilite. As the temperature decreases, this Na_2SO_4(V)-$Na_2SO_4 \cdot 10H_2O$ solubility ratio increases rapidly which will impact the kinetics of crystallization as a solution supersaturates [8]. For example, in porous construction materials contaminated with sodium sulfate, exposure to moisture will cause thenardite to dissolve, but the solution will become supersaturated with respect to mirabilite before thenardite at lower temperatures. This will lead to the crystallization of the hydrate and potential damage of the material as the hydrous crystal structure is larger than the anhydrous phase. The lower the temperature, the greater the discrepancy in solubility and the more mirabilite with crystallize, generating greater pressures and therefore causing increased damage.

Figure 2 presents a simplified version of the phase diagram for sodium sulfate that effectively describes the most important phase changes of sodium sulfate for the current research. The phase diagrams show that at room temperature (ca. 20˚C) sodium sulfate is present as thenardite unless a high relative humidity is reached, specifically between 76.4-95.6%, at which point mirabilite becomes the stable phase [8]. During the drying process of a solution at room temperature, from the phase diagrams in Figure 2 and Figure 3the theoretical thermodynamic pathway would be the precipitation of mirabilite followed by dehydration to thenardite. Experimental studies performed by Steiger and Asmussen, showed that other phases (such as the heptahydrate, the anhydrite III and V) can precipitate directly from solution as well [8]. At a relative humidity below ca. 76%, lower temperatures can also cause the phase shift from thenardite to mirabilite.

When applied to the case of a porous building material contaminated with sodium sulfate, the damaging potential of changing humidity conditions was investigated by Desarnaud et al. [6]. This study focused on the kinetics of salt crystallization and with their experimental process found that while wet/dry cycles with liquid water lead to a crystallization process that induces damage in the stone tested, humidity cycles did not. This renders humidity testing less effective when using sodium sulfate. Despite reaching supersaturation, the growth period of the hydrated salt during relative humidity cycling was brief and the crystals would subsequently dissolve resulting in an homogeneous solution. Thus, large crystallization pressures did not develop. In contrast, dissolution-crystallization cycles with liquid after the initial salt contamination formed heterogenous solutions within the specimens. As the dehydrated thenardite crystals began to dissolve, the solution reached supersaturation with respect to mirabilite even before all the thenardite dissolved. Additionally, crystals likely develop quickly within in all pore sizes preventing the thenardite-mirabilite equilibrium from being maintained [5]. The remaining thenardite crystals provide nucleation sites for mirabilite which was observed to crystallize more rapidly, leading to higher crystallization pressure [6].

2.2.2 Physical characteristics of porous building materials in relation to salt damage

Porous building materials such as stone, brick, mortar, and concrete have unique intrinsic characteristics that will impact the way salt crystallization-dissolution processes will affect their material integrity. As previously mentioned, the level of damage that salt can cause depends on several factors such as the type and amount of slat, environmental conditions and, of course the material properties, namely the porous structure and mechanical strength [5].

The porous structure of a material can be described by several parameters such as the open porosity, pore size distribution (PSD), density, and specific surface area. The study of these characteristics is fundamental to understanding water transport within their network [16]. This, in turn, is necessary for understanding the impact of salt crystallization. It is the crystallization-dissolution and re-mobilization of salts that lead to the development of damage [3].

Liquid water can be transported though porous media by capillary action, which is one of the most important mechanisms when studying the interaction of water with porous building materials. At the atomic level, it is governed by the relationship between the attractive forces within water (cohesion) and the attractive forces between the inorganic material and water (adsorption). These attractive forces result from the polar nature of water and mineral molecules in porous materials. The movement of water into pore networks is continued by the attraction of water molecules to ‘dry’ surfaces further along the pore channels [17].

The relationship between cohesive and adsorptive forces that describes the capillary phenomena is also affected by the size of the pores within the porous building material. The hydrogen bonds that water can form with other polar molecules is not very strong (compared to ionic and covalent molecular bonds). Therefore, only water molecules close to the pore walls are affected by the adsorption effect. Due to this, smaller pores can draw water further into their network, but larger pores transport water more

quickly due to their larger cross-section [17]. The rate of liquid this water transport can be described by the capillary absorption coefficient [18]. Researchers Angeli et al. have suggested that this coefficient is the most important parameter for predicting durability as it relates to the ease of migration of a solution into the pore network [19]. In their study, they found linear correlation between the capillary absorption coefficient and the Alteration Index (defined as the number of cycles it takes for damage to first be observed [4]).

Other factors (capillary condensation and gravity) dominate when pore sizes are larger or smaller than the capillary pore range, preventing the mechanisms of capillary action [17]. The range of capillary pores, from ca. 1mm to a few nanometers, is thus named because capillary action is the governing mechanism (Figure 4). Most inorganic building materials pore sizes are within the capillary pore range [8] [17].

<table>
<tr><td>Macropores</td><td colspan="2">Micropores</td><td colspan="2">Nanopores</td></tr>
<tr><td>> 1 mm</td><td>1 mm – 10 µm</td><td>10 µm- 0.1 µm</td><td>100 nm- 10 nm</td><td>< 10 nm</td></tr>
<tr><td>Liquid water flow</td><td></td><td></td><td></td><td></td></tr>
<tr><td></td><td colspan="2">Capillary absorption</td><td></td><td></td></tr>
<tr><td></td><td></td><td colspan="3">Water vapour adsorption and surface diffusion</td></tr>
<tr><td></td><td></td><td></td><td colspan="2">Capillary condensation</td></tr>
<tr><td colspan="3">Water vapour diffusion</td><td></td><td></td></tr>
</table>

Figure 4: Water transport mechanisms depending on pore diameter [17]

Aside from affecting the mechanics of liquid transport, the pore size distribution also influences the susceptibility of a material to damage from salt crystallization. Several experimental and theoretical studies demonstrated that crystallization pressure increases with the decrease of pore size [9]. Therefore, materials with a large fraction of micropores, are more vulnerable to salt attack [5]. Yu and Oguchi developed a durability estimator called the salt susceptibility index (SSI) based on this concept [20]. The estimator combines several factors related to pore size and connectivity to develop this ranking metric. However, this study also noted that pore size is not the sole contributing factor to salt decay. The impact of the overall porosity, capillary absorption, connectivity of the pore network, pore shapes, and specific surface area, all need to be considered to interpret the durability of stones [5].

While capillary absorption is a relatively rapid mechanism, evaporative drying is slower and governed by different transport processes throughout the different stages of drying. When a porous material is saturated, water will evaporate from the surface (i.e. the evaporation front is located at the surface); capillary transport will continue to draw more liquid to the exterior until a critical moisture content is reached and capillary transport is inhibited. Subsequently, drying through vapour diffusion becomes the most important mechanism. Since porous construction materials are not homogeneous, there will be a transition phase where drying will be governed by a combination of both mechanisms (capillary and

vapour diffusion), during which the evaporation front will recede into the material. Finally, when no liquid water remains, drying will be dictated solely by vapour diffusion, which is a very slow process. Vapour diffusion will continue until water from the porous structure is completely depleted, or until the residual moisture content (determined by the environmental conditions) is reached [17].

In the presence of soluble salts, as the drying of a porous material progresses, the movement of salt will become increasingly restricted. Firstly, salts will be drawn by capillary action towards the surface where evaporation takes place. The re-mobilization of salt during drying leads to the development of salt gradients in the medium [19]. Once the drying process reaches the critical moisture content, transport of salts is greatly reduced, although it is not completely restricted. Layers of water that are adsorbed into the pore walls can still dissolve and transport salts, a phenomenon known as salt creep, which even allows salt movement below the relative humidity equilibrium. Due to the hygroscopic nature of soluble salts, they self-contribute to their own transport within a material because they attract and hold moisture in their structure. This hygroscopic nature of salts is the main cause for the reduction of the drying rate of salt contaminated materials [17].

The dynamics of evaporation is a factor of outmost importance in the resulting level of damage. As confirmed by Angeli et al. [19] from their comparison of damage induced by partially immersion and total immersion of specimens with 3-4 sides sealed. While both the surfaces of the samples covered by solution in the partial immersion test and the sealed faces of the sample from the complete immersion test experience complete saturation with the salt solution, only the capillary samples and the exposed surfaces of the immersion samples showed damage. This indicates the importance of evaporation to the development of damage. It concluded that the more opportunity for evaporation leads to faster development and greater damage.

The mechanics of capillary transport, evaporation, and vapour diffusion within the material combined with all the physical properties of a pore network all need to be understood if an accurate and realistic prediction is to be made. Additionally, when considering the durability assessment of materials already in a construction, the existing state of the material must be considered. Weathered and sound stones from a quarry may have a very different, as for instance biological presence, patinas, and past deterioration from weathering can change the ‘breathability’ of the material and affect the water and salt transport mechanism [3]. Finally, the additional variability and complexity the many environmental factors discussed can have on accelerated salt aging tests during wet and drying processes makes the development of simple yet realistic and effective testing standard a challenge.

3. METHODOLOGY

3.1 Stone Characterization Tests

3.1.1 Capillarity Absorption Test

The water absorption by capillarity curves and the calculation of the absorption coefficient of each stone was determined following the experimental procedure for 'Penetration of Water: Capillary Action' detailed in [21]. Three specimens of each type of stone were placed in a container on top of a mesh and distilled water was added to the height of 2-3mm up the sides of the stone. The stones were weighted at regular intervals and the water front was registered as time progressed. As some of the stones showed a very slow absorption rate, readings were continued up to six days depending on when the stone finally reached a stable saturation level. This also allowed for the determination of the maximum absorption capacity of the three types of stone.

3.1.1 Drying curve at 50% RH

The drying curve was determined according to RILEM 25-PEM [18] for each of the types of stone used in this research to help in the analysis of the accelerated aging tests. Three samples from each lithotype were used. They were first immersed in distilled water until saturation, then all but the top face was sealed using plastic wrap and tape to ensure unidimensional evaporation. The stones were placed in an environment with 50 ±5% relative humidity and a temperature of 20 ±2˚C. The weight of the specimen was recorded several times within the first eight hours of drying and subsequently every 24h (excluding weekends) until the moisture content in the stones stabilized.

3.1.2 Drying Test at 50% RH with salt impregnated samples

To study the effect of salt on the drying behaviour of the stones, the same drying test as described in 3.1.1 was conducted with the same specimens, but using a salt solution of 14 w.t. % $Na_2SO_4 \cdot 10H_2O$ instead of distilled water to saturate the stones.

3.1.1 Oven Drying Speed

The drying speed of Božanov and Mšeno was tested to ensure, the selected time for drying in the new aging test would be sufficient for most of the water mass (>80%) to evaporate. As Opuka was added to the experiment after the procedure had been set, its drying speed was not analyzed. The test was conducted by immersing six samples of each stone in distilled water for 2 hours. Then three samples of each stone were placed in an oven at 40˚C and the other three samples in an oven at 60˚C. After two hours of drying, the samples were removed and weighted so the remaining water content could be determined. The stones were replaced in the oven to continue drying overnight and were again weighted after more then 20 hours of drying.

3.2 Accelerated Salt Aging Test

The accelerated aging test was designed based on the existing EN 12370 standard for *Determination of resistance of natural stone to salt crystallization*. This norm entails conducting multiple cycles of stone sample immersion in sodium sulfate followed by drying in an oven for at least 16 h [12]. In practice, a salt crystallization test should reflect the real materials and material combinations in heritage constructions, however the scope of this research focuses on the performance of stone materials solely. Although the concepts can be transferred to the assessment of other materials such as brick, the evaluation of compatibility of material combinations (e.g. combination of mortars and masonry units) requires further consideration [3].

This research was based on EN 12370 experiment and 4 variations of this procedure were designed. The specimens used in all the tests were cut into cubes with side dimensions of approximately 5 cm. All the stone specimens were then washed to remove debris and dried in a ventilated oven at 60˚C until they reached constant mass. Each sample was labeled and weighed to establish its initial undamaged dry weight. In total, twelve cycles of wetting and drying were carried out for all five of the experiments. Following is a description of the five different procedures, and a summary of all the procedures is provided in Table 1.

Test Procedure 1

This procedure follows the EN 12370 standard and each subsequent procedure is derived from modifying this baseline process.

In each cycle, samples were completely submerged for 2h in 14 wt.% sodium sulfate decahydrate ($Na_2SO_4 \cdot 10H_2O$) ensuring they were covered by ca. 10mm of salt solution. Each sample was placed in its own container, which was covered with plastic wrap during immersion to prevent evaporation (Figure 5). After wetting, the samples were weighed and placed in an oven at 40˚C and an initial high relative humidity (RH) achieved by placing approximately 350mL of water in a pan at the bottom of the oven. At 2 h intervals, the temperature (T) of the oven was increased to 60, 80 and 105˚C. Once at 105˚C the samples were left overnight to dry at this temperature. The next day, the specimens were removed from the oven and left to cool in a desiccator for an hour at which point their new dry weight was recorded before beginning the next cycle.

Test Procedure 2

In this variation, samples were submerged in 7 wt.% $Na_2SO_4 \cdot 10H_2O$. The rest of the procedure, drying times, and temperatures were the same as in Test Procedure 1.

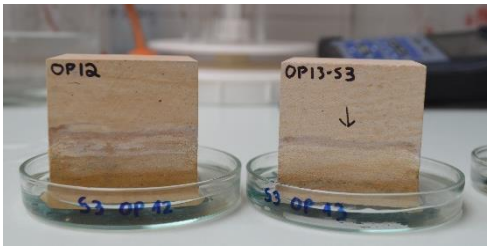

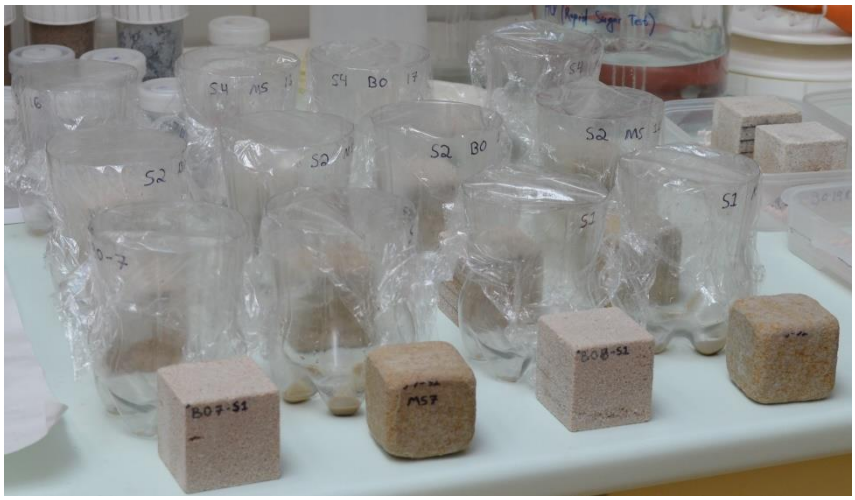

Figure 5: Wetting Phase

Top Left – example of samples during immersion.

Top right - example of capillary samples.

Bottom - preparation for immersion with plastic covering

Test procedure 3

Contamination with the salt solution was achieved via partial instead of complete immersion. In each cycle samples were placed in a Petri dish with 3(±1) mm of solution for 2h. In the 1st, 5th, and 9th cycles this solution was 14 wt% $Na_2SO_4 \cdot 10H_2O$. In all other cycles, the stones were simply re-wetted with distilled water. To limit salt solution evaporation from the Petri dishes, the samples were covered with a plastic container during the wetting period. After wetting the samples were dried in the same process as in Test 1.

Test procedure 4

Test Procedure 4 once again used 14 wt% $Na_2SO_4 \cdot 10H_2O$ solution and contaminated the specimens through 2h of total immersion. The variation came in the drying process. After the wetting phase, the samples were placed in an oven at 40˚C, providing an initial high RH same as for the other test procedures. However, after 2h, the temperature of the oven was increased to 60˚C, instead of 105˚C, and the samples were left overnight to dry at this temperature.

Test procedure 5

The final procedure conducted combined all the variation of Test 1 seen in Test Procedures 2-4. A solution of 7 wt% $Na_2SO_4 \cdot 10H_2O$ was used and contamination was achieved through partial immersion. Re-wetting of the samples was done with salt solution in cycles 1, 5, and 9, but only distilled water in all other cycles. Finally, overnight drying of the specimens was carried out at the lower temperature of 60˚C (after the initial 2h at 40 ˚C).

Reference Test

A reference test where specimens were only exposed to distilled water was also conducted. In each cycle, samples were submerged for 2h in distilled water ensuring they were covered by ca. 10mm of water. The immersion containers were covered to prevent evaporation. After wetting, the samples were weighed and placed in an oven at 40˚C and an initial high RH achieved by placing approximately 350mL of water in a pan at the bottom of the oven. A reference sample for each of three types of stone was dried according to the drying phase described for procedures 1-3 (high T - 105˚C), and one sample was dried according to procedures 4-5 (low T - 60˚C).

Additional procedural details that applied to all the tests include the following:

- If the cycles could not be continued the following day, the specimens were left in the oven at their respective drying temperatures.
- At intervals of 4 cycles, testing would be done on the specimens to monitor their deterioration (as described in section 3.3.3), on these days the specimens were stored in a desiccator at room temperature.

Table 1: Summary of testing procedures for accelerated aging tests

Procedure	Exposure Method	Concentration of Salt (w.t.%)	Rewetting	Drying Conditions
R	Immersion	0%	All Cycles - Water	Samples for both conditions
S1	Immersion	14%	All Cycles - Salt	Start 40˚C increase to 105˚C
S2	Immersion	7%	All Cycles - Salt	Start 40˚C increase to 105˚C
S3	Capillary rise	14%	Cycles 1, 5, 9 – Salt Other cycles- Water	Start 40˚C increase to 105˚C
S4	Immersion	14%	All Cycles - Salt	Start 40˚C increase to 60˚C
S5	Capillary rise	7%	Cycles 1, 5, 9 – Salt Other cycles- Water	Start 40˚C increase to 60˚C

The EN12370 standard was established almost 20 years ago, and is still used today, but investigating the variations detailed in the five test procedures above have been done with the aim of moving towards a more realistic testing procedure. As stated in [3], an effective laboratory aging test should reliably simulate the in-situ behaviour of the material being tested, but within a short period of time.

In light of this, the exposure paths of partial versus complete immersion were considered. Most buildings and monuments are never completely immerged in salt solution, although it is recognized exceptional building circumstance or flooding can occur in certain areas that may cause this. However, this is considered the exceptional circumstance; in the majority of situations building materials are exposed to moisture (and salts) from the ground (rising damp) and/or rain. The distribution of salt within constructive elements depends on the contamination method, and the same applies to laboratory experiments (e.g.

partial versus complete immersion). Hence, both partial and total immersion procedures were considered in this work.

Salt concentration is another factor of major importance in the degradation process. The concentration of salt was reduced to 7wt.% for some of the procedures. This was also done because such high concentrations (14wt.%) are not realistic [3]. As mentioned in the methodology, high concentration of salt solution may even induce damage that is not seen in real building.

It is for these same reasons that re-wetting with water was also considered. In the natural environment many sources of moisture, such as rain, ground water, and high RH often wet masonry materials without introducing more salt, yet damage still develops. Studies have shown that even simple re-wetting and re-mobilizing sodium sulfate can cause damage without additional salt [6].

The stipulated contamination time prescribed in the EN12370 standard (2 h) was maintained in all the test procedures. Complete drying after re-wetting helps accelerate damage, but ensuring that at least 80% of the water introduced has evaporated can be considered as effective and has the advantage of reducing the testing time [11].

Drying at the extremely high temperature of 105˚C as prescribed in the EN12370 standard is not in line with any thermal conditions occurring in the real environment. Drying temperature influences where and how salt crystallizes. Under natural environmental conditions, salt usually accumulates close to the surface. If the drying temperature is too high, the drying rate will increase and salt will tend to crystallize in the interior of the stone leading to internal damage in the stone, which is not a damage mechanism seen in-situ [3]. For stones and/or other masonry components under testing that are shown to lose most of their water content after drying at a lower temperature, using a reduced temperature would better simulate in-situ conditions. Moreover, in a study on the crystallization phases of sodium sulfate by Steiger & Asmussen, was able to attain results with 12 hour drying cycles, even at a temperature of 27˚C with a dry atmosphere [8]. Therefore, more realistic thermal conditions should be achievable in a laboratory test. To this end, the drying temperature was modified to 60˚C for some of the test procedure. A temperature of 40˚C was initially proposed, however due to limited availability of ovens, a temperature of 60˚C was used.

Other variations, such as relative humidity cycling, was not investigated following evidence of the lack of efficiency of this process in developing crystallization pressure when using sodium sulfate, as mentioned in the state-of-the-art [6].

As previously mentioned, it is known that the process of dissolution-crystallization causes damage with sodium sulfate, therefore more cycles would cause more damage. But, due to limited time for the experiments, only 12 cycles were feasible to perform.

3.3 Monitoring and Deterioration Analysis Tests

3.3.1 Visual Observations

To help document the deterioration of the specimens and the alteration in their visual aspect, visual observations were made during each cycle. Additionally, photographs of the specimens were taken at the end of each drying stage to document the damage caused during the previous cycle.

3.3.2 Mass Evolution and Mass Loss

The mass of each specimen was carefully monitored throughout the entire experiment. The initial dry mass and subsequent dry mass of the specimens after each drying phase was measured on a digital balance with resolution of 10^{-3} g and accurate to 10^{-2} g. Additionally, the saturated weight after the wetting phase was also recorded in each cycle.

Material loss during the wetting, drying, or intermediate phases, was carefully tracked. Any large losses of material during drying or while handling the samples between the experimental stages was collected, measured, and recorded. However, within each cycle the mass losses from general handling were very minute and therefore neglected.

During wetting, each specimen was placed in its own container allowing for easy collection of the mass lost in this phase. At intervals of four cycles, the lost material from each stone was decanted from the remaining salt solution, rinsed with distilled water to remove the salt, and then put in smaller containers to dry in the oven until constant mass. Figure 6 shows an example of the collected and dried material. For the samples that were used in the ultrasonic testing described in section 3.3.3, the mass loss during desalination was also collected, dried, and weighed.

Figure 6: Example of collected and dried mass loss during wetting

3.3.3 Ultrasonic Testing

Ultrasonic pulse velocity (UPV) testing was used to help track the progression of damage in the different specimens. In the past, several research studies have attempted to relate the UPV to various stone properties such as mechanical strength, porosity parameters, density, and for used the determination of the dynamic modulus of elasticity [22]. It can also be used to assess the level of weathering or

deterioration in stones. The velocity of ultrasonic waves is affected by inelastic and elastic properties. The main properties include the stones mineralogy, physical properties (porosity, pore space, density), mechanical properties (strength), the degree of water saturation and the level of deterioration [22]. Many of these properties can be affected due to damage induced by salt crystallization cycles. Measuring the UPV after salt weathering can help provide insight into the degree of damage inflicted. As referenced in [22] the researchers Chiesura et al. highlighted that ultrasonic test data alone cannot provide a full picture of the deterioration.

The ultrasonic equipment used in this work was a USG 20 device with a 250 kHz vibrator (USG-T) and receiver (USE-T). The transmission mode technique was used: one transmitter and one receiver. Testing was conducted on one of each stone types per testing procedure except for the reference (water aged) samples. Using a pencil, reference lines were drawn on one of the side faces of each specimen dividing it into five 1cm sections. A measurement was taken at the center of each of these sections, resulting in five measurements per sample. Measurements were taken before starting the contamination cycles to characterize the stones in their sound state. Subsequent measurements were taken after 4, 8, and 12 cycles, and finally after desalination. Desalination was carried out by immersing each sample in distilled water and changing out the water once or twice a day to rinse the salt out of the stone's fabric as best as possible. To accelerate the desalination process and prevent further damage due to the hydration of thernadite to mirabilite during wetting, the specimens were submerged in water at a temperature of 40˚C and placed in an oven to maintain this temperature.

3.3.4 Salt Distribution

The distribution of salt within the stone specimens was investigated using the properties of electrical conductivity of saline solutions. One sample from testing procedures 1, 4, and 5 were selected for each of the three stone types. A rectangular core with a 1cm by 1cm cross section was saw-cut (without water) from the center of each of the cubes selected. This core was then divided into slices with a thickness of 5mm. Since the specimens have ca. 5cm length, theoretically, 10 slices should be obtained. However, due to the thickness of the saw blade used to cut the samples only 7 slices were obtained (Figure 7).

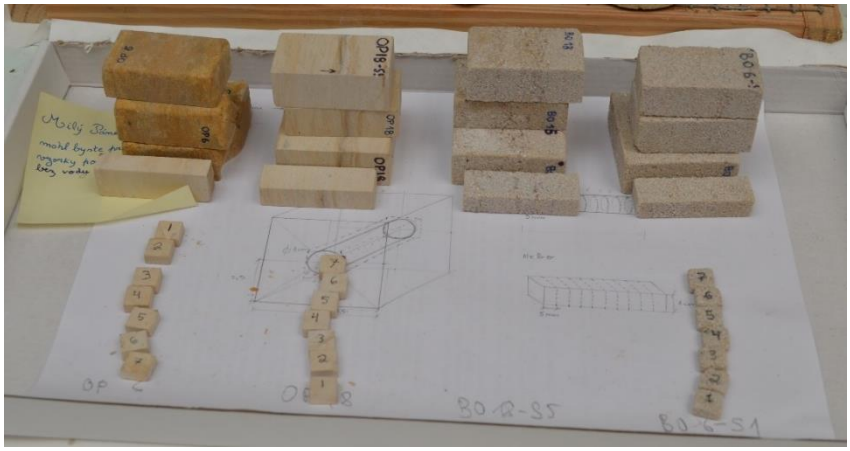

Figure 7: Cut samples for the salt distribution analysis

Each of these specimens was ground into a fine powder and mixed with ca. 50mL of distilled water to solubilize the salt present in each slice. Each solution's conductivity was measured, from which the concentration of salt in each stone slice was determined. With this data, the influence of each ageing test procedure on the salt distribution within the stones could be evaluated.

The stones can have exchangeable ions that might contribute to the conductivity of the solutions. Therefore, samples of the reference stones were also taken, crushed, mixed with distilled water and their conductivity measured. With this baseline information for each type of stone, a more accurate measure of the salt concentration in the contaminated samples could be made.

A suitable conductivity curve of sodium sulphate adaptable to this study was not found in the literature. Therefore, one was developed by preparing solutions of $Na_2SO_4 \cdot 10H_2O$ with concentrations at 0.01% steps ranging from 0.00-0.10wt%. Their conductivities were measured and a linear relationship was established to correlate concentration and conductivity. The conductivity curve and linear relationship developed from this data can be found in Appendix A: Sodium Sulfate Decahydrate Conductivity Curve.

3.3.5 Microstructural analysis using the Scanning Electron Microscope

Microscopic analysis of select specimens was conducted to analyse the morphology and distribution of sodium sulphate within the stone's structure. A MIRA II LMU (Tescan corp., Czech Republic) scanning electron microscope (SEM) equipped with energy dispersive X-ray detector (EDX) from Bruker Corporation (Germany) was used. The Back-Scatter Electron (BSE) mode was used as the secondary electron (SE) was causing over charging of the specimen surface. The EDX facilitates elemental mapping and point analysis for a deeper investigation of the salt distribution within the specimens.

SEM observations were performed on a freshly fractured cross section of each stone specimen (ca. 5mm thickness). This allowed the observation of the morphology of the exterior surfaces and interior matrix of the stones close to the surface. The samples were then coated with gold and observed under the SEM. The images were collected under high voltage (15 kV) at a working distance of 15mm and under high vacuum regime. Samples for each test procedure and stone type were analysed with the aid of an expert in geology and microscopic analysis.

4. RESULTS AND DISSCUSSION

4.1 Stone Characterization

4.1.1 General Characteristics

Three types of stone were selected for this study: Božanov sandstone, Mšene sandstone, and Opuka marlstone. Apart from having been widely used in the past in the construction of monumental buildings in the Czech Republic, they are also still recurrently used in restoration interventions [23] [24]. Therefore, the selection of these stone types was based both on their distinct properties, namely regarding their porous structure and mechanical strength, and on their importance in architectural heritage conservation. In a recent Czech national project (NAKI18) in which ITAM was a partner, several properties of specimens extracted from the same stone blocks used in this work were determined [25]. Some of the results from this project were used in this work.

Božanov

Božanov is a grey sandstone with beige-brownish spots (Figure 8). It is a locally quarried stone and commonly used historically in buildings and monuments in the Czech Republic [26]. It is a mid-grain, extremely hard silicate sandstone with a high level of diagenesis [27]. Similar to other sandstones it is composed of quartz clasts, tourmaline, epidote, muscovite, and zircone [26]. Figure 9 shows an image and the composition of Božanov's grains and binder from a SEM analysis. From the elemental analysis, it is known that silica and aluminum oxide are the two most prevalent components.

Figure 8 : Example of Božanov stone - visual characteristics

Božanov exhibits a relatively strong compressive strength of ca. 53.1 MPa and a bending strength of 5.8MPa [26]. The porosity and water transport properties of Božanov and the other two stones are discussed in detail in the following sections

Elemental Analysis		
Compound	***BO5-2***	***BO5-3***
CaO	1.04	0.54
SiO2	61.75	60.49
Al2O3	30.42	26.84
MgO	2.38	3.34
Na2O	0.05	0.31
K2O	2.84	4.72
FeO	1.51	3.77
Total	99.99	100.01

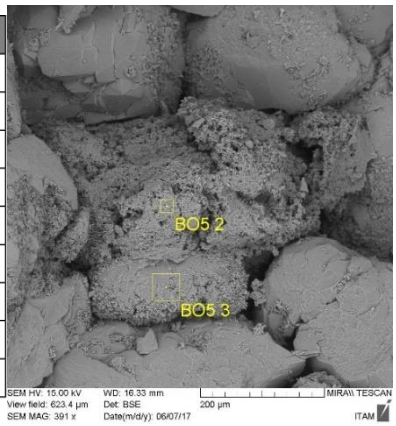

Figure 9 : SEM of Božanov grains and binder

Mšene

Mšene is a type of sandstone from the Czech Cretaceous Basin, mined at the Mšené-lázně quarry located northwest of Prague [28] [25]. It is another stone that has commonly been used in architecture and sculptures in Prague including in the construction of St.Vitus's Cathedral at Prague Castle, the Ministry of Finance, the Ministry of Trade and Industry, and in the restoration of monuments such as Our Lady with Saint Dominic and Saint Tomas Aquitanus sculptures in the Charles bridge [28]. Petrographically classified as a strengthened sediment, Mšene is a fine grained (0.25-0.05mm) calcite-

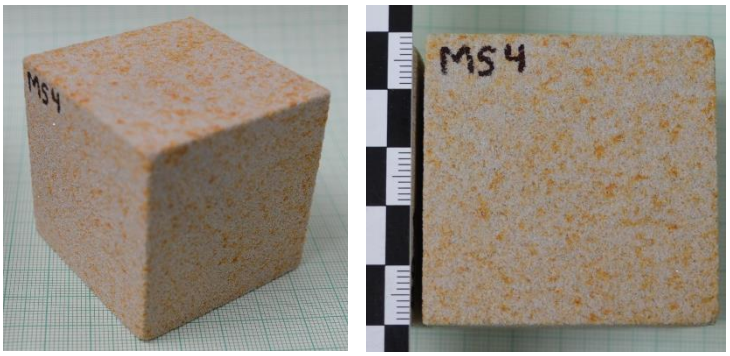

Figure 10: Example of Mšene stone – visual characteristics

Table 2 : Mineralogical composition of Mšene [23]

Component	Quantity
Quarts	99.6%
Feldspar	0.2%
Muscovite	0.1%
Chlorite	0.08%

argillaceous sandstone of white-grey colour with yellow to brownish spots (Figure 10) [28] [25]. It is a monomict, equigranular stone mainly composed of quartz with minor contents of clay and other minerals (such as muscovite) interspersed [25] [28]. The clay intrusions were detected during analysis with SEM-EDX and are shown in Figure 10. The mineralogical composition using X-ray diffraction as determined in [23] is given in Table 2 . Mšene stone was the focus of the study by Zbyšek et al. [28] that concluded its large pores mean its susceptibility to salt damage is low and therefor it is suitable for use in severe environmental conditions. Mšene sandstone has a compressive strength of 23MPa when dry, which is reduced to 19MPa when saturated with water [23].

Elemental Analysis	
Compound	***MS6-3***
SiO2	55.09
Al2O3	43.27
Na2O	0.08
FeO	1.55
total	99.99

Figure 11: SEM of a clay particle in a sample of Mšene sandstone

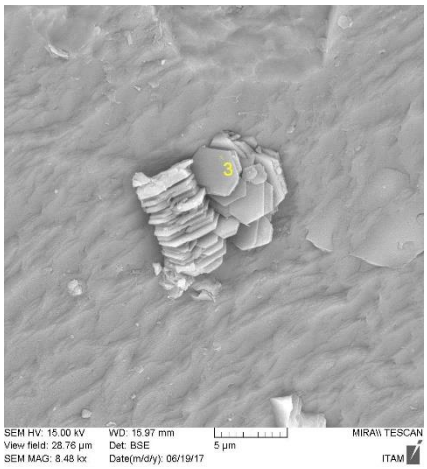

Opuka

Opuka stone has commonly been used in historic times in Prague and central Bohemia in buildings and sculptures as it was readily available from local quarries [29] [30] [31]. Opuka stone has also been the focus of several research studies and widely used in restoration projects as it's deterioration due to environmental factors has caused urgent and serious [29] [31].

Figure 12: Example of Opuka stone – visual characteristics

The characteristics of Opuka stone were studied in detail by researchers from Charles University, who classified it as a marly chert [30]. Other sources describe this marlstone as a 'clayey siliceous micritic limestone' belonging to the Upper Cretaceous sediments of Bohemian Cretaceous Basin [32]. Opuka is an extremely fine-grained stone, with light beige to yellowish colouring (sometimes described as golden or ochre [30] [32]) and often marked laminations [29] (see Figure 13). It is important to note that all tests and experiments in this research were conducted parallel to these distinct bedding planes that show the different sedimentary layers. A complete characterization of Opuka stone should also analyse the stones properties perpendicular to the bedding layer. However, for the purpose of this research only the orientation parallel to the laminations, which is the most likely orientation adopted in constructions, was considered.

Table 3: Mineralogical makeup of Opuka Stone [as referenced in [22]]

Component	Quantity
Quartz	50.3%
Calcite	28.1%
Mica	11.2%
Kaolinite	8.8%
Pyrite	0.1%
Geothite *	1.2%
Rutile & anatase	0.3%
Potassium feldspar	Traces

***Gives the stone it's ochreous colour**

The mineral makeup of Opuka stone was determined by Pavlik, et al. [30] and a summary is given in Table 4. In this work, samples were also analysed with SEM-EDX. Other properties of Opuka stone in the sound condition include [32] [29]:

- Density: 2.65 g/cm^3
- P-wave velocity: 1.97 km/s
- Uniaxial compressive strength: 65.2 MPa
- Tensile Strength: 5-7 MPa

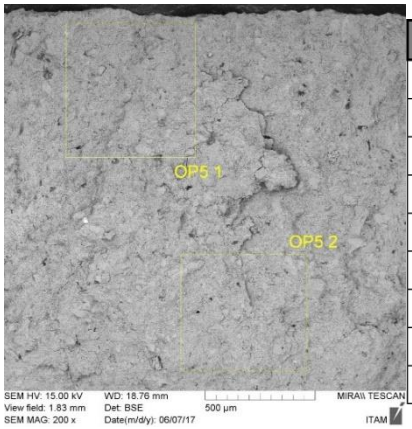

Elemental Analysis		
Compound	***OP5-1***	***OP5-2***
CaO	16.63	16.16
SiO2	71.12	69.68
Al2O3	8.6	9.03
MgO	0.17	0.12
Na2O		0.12
K2O	0.87	0.92
FeO	2.62	3.98
Total	100.01	100.01

Figure 13: SEM EDS analysis of Opuka stone

4.1.2 Porosity and density

Open porosity, water absorption, and bulk density

The results from NAKI18 [23] on bulk density, open porosity, and water absorption coefficient of Božanov, Mšeno, and Opuka stones are shown in Table 4. The tests were performed using three samples of each stone type with dimensions of 50 x 50 x 50 mm.

Table 4: Physical properties of Czech stones determined in the NAKI18 project [25] the values are the average (±standard deviation)

Stone Type	Water absorption at atm. pressure		48 at vacuum, RILEM Test No. II.2.		
	24 h [%]	48 h [%]	Bulk density [kg.m^{-3}]	Open Porosity [%]	Water absorption [%]
Božanov	4,8 ± 0,2	4,9 ± 0,1	2167,7 ± 10,5	17,4 ± 0,4	8,0 ± 0,2
Mšeno	12,0 ± 0,2	12,3 ± 0,2	1861,9 ± 12,2	29,7 ± 0,4	15,9 ± 0,3
Opuka OV (parallel to bedding)	8,2 ± 0,1	9,4 ± 0,6	2045,0 ± 28,7	23,5 ± 0,8	11,5 ± 0,6

From the data presented in Table 4, it is observed that Mšene has the highest open porosity (ca. 30%), followed by Opuka (ca 24 %). In contrast, Božanov shows the lowest open porosity (ca. 17%). In terms of absorption capacity, the same order or ranking applies. Regarding the results of water absorption at atmospheric pressure and under vacuum (48h), the standard deviation for Opuka is usually the largest, which indicates its higher heterogeneity in comparison to the two sandstones. As the amount of salt uptake depends significantly on the porosity of the stone, these differences are likely to influence the level of damage. The relative difference in the percentage of open porosity is also reflected in the differences in bulk density of the three stones.

Table 5: Solid Density Properties of samples - NAKI18 project [23]

Stone Type	Solid density [kg/m3]
Božanov Sandstone	2637
Mšené Sandstone	2897
Opuka	2672

Pore Size Distribution

The NAKI18 project conducted by ITAM investigated the pore structure of several stones types using the Mercury Intrusion Porosity (MIP) method [25]. From this study, the characteristic pore size distribution (PSD) curves for Božanov, Mšeno, and Opuka was determined and is shown in Graph 1.

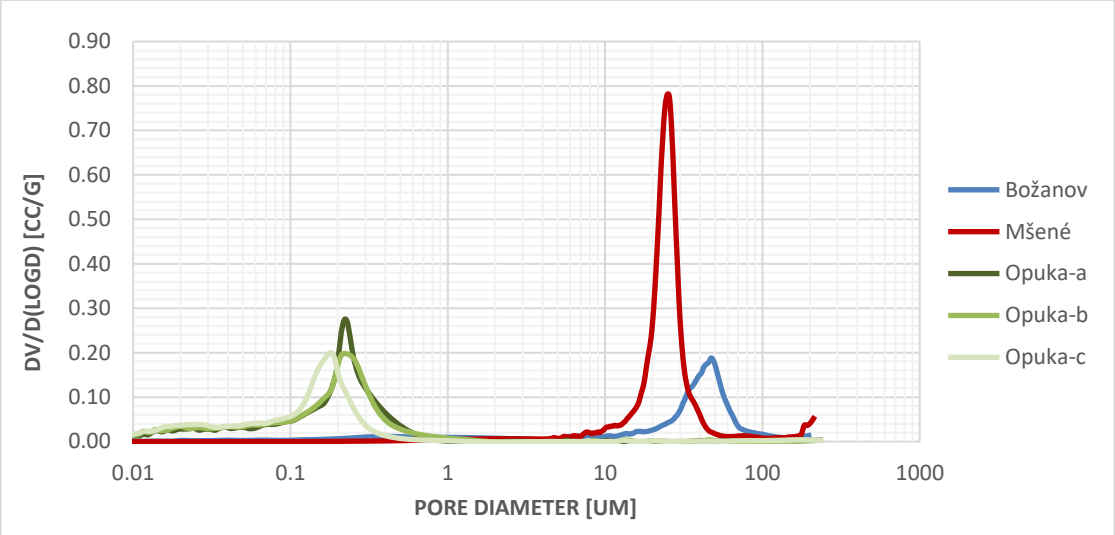

Graph 1: Pore size distribution for Božanov, Mšeno, and Opuka stone (adapted from [25])

The PSD curves (Graph 1) show that all the stone types have a monomodal distribution. The porous structure of the two sandstones (Božanov and Mšeno) is mainly characterized by capillary active pores (Fig. 4). Opuka stone shows a main PSD maxima at ca. 0.2μm, but a portion of the pore volume is in the range from 10 to 100nm, which can have an important effect in salt deterioration processes. Although the sandstones have similar PSD in comparison to Opuka, Božanov's pore volume maxima is approximately twice the diameter of Mšene's. According to the IUPAC classification of pore sizes [33], all stones have macroporous structures as their pore diameters are higher than 50nm. Some authors [34] [35] have criticized the IUPAC classification and given alternative pore size classifications. With respect to the stones under study in this work, the macropore classification does little to indicate the difference in physical behaviour that will likely be seen in particular between Opuka and the two sandstones as their pore size differ by two orders of magnitude. Mays [35] suggests nomenclature more in line with the SI terminology that would classify Opuka as sub-microporous and Božanov and Mšeno as sub-microporous. Although this system may provide more detailed division and classification of pores based on their size, it's subdivisions give no indication to the differences in physical behaviour, with respect to absorption or evaporation kinetics like those provided previously in Figure 4.

As capillary action and water movement within the stones is largely dependent on their pore size distribution, the difference in size and quantity of pores between the three types of stones will cause distinct behaviours in absorption, drying, water movement, and of course, salt transport [17]. These different behaviors are discussed in more detail in following sections.

4.1.3 Capillarity Absorption Test

Graph 2 to Graph 4 show the water absorption by capillarity curves for each stone. The water absorption by capillary coefficient was calculated according to EN1925, and the average value for the three types of stones was determined. This data, along with the results of the NAKI18 project [25] are presented in Table 7.

The graphs clearly show that Mšene has the fastest absorption rate, while Opuka's absorption rate is significantly slower than either of the other stones. Mšene samples reached the capillary moisture content, i.e. amount of water absorbed by the sample sufficient to wet the upper surface by capillary rise from the bottom, within one minute of starting the test. The calculated capillary absorption coefficients (Table 7) support these observations; Mšene has an average coefficient of 58.3±2.3 kg/m^2 h^{½}, while Opuka has the lowest coefficient (ca. 2.2 kg/m^2 h$^{-½}$). However, from the graphs it is seen that Mšene and Opuka have a similar maximum absorption capacity within 9.8-10.4 kg/m^2 and 10.5-10.8 kg/m^2, respectively. Božanov is the odd one out in this respect, leveling off with a maximum absorption capacity between 4.29-4.54 kg/m^2.

The spread between the three samples of Opuka overall is very small, which can visually be seen in Graph 4 and is confirmed by having a very small standard deviation (SD). For the three samples of Božanov there is a notable variance in the time it took for each specimen to reach complete saturation therefore it's absorption coefficient has the largest standard deviation at ±3.12 kg/m^2 h^{½}. However, once fully saturated the spread between he maximum absorption capacities of the three stones was very close. For the Mšeno

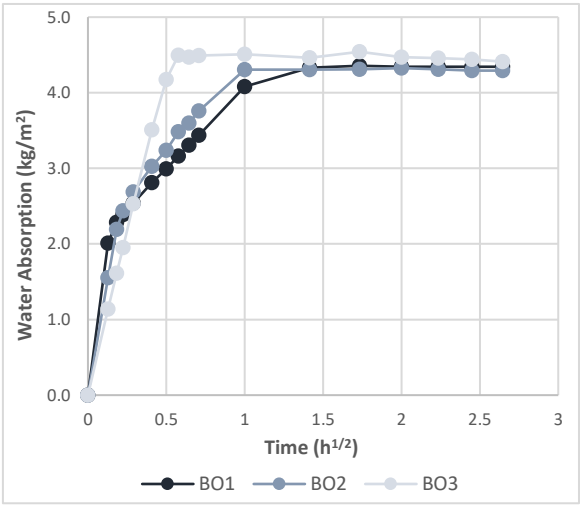

Graph 2: Capillary absorption - Božanov stone

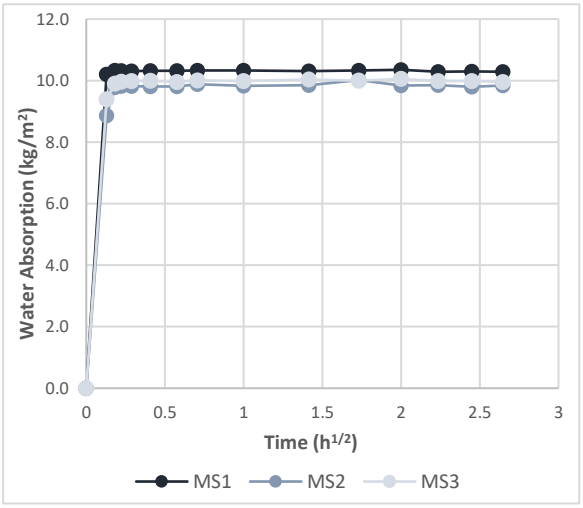

Graph 3: Capillary absorption - Mšene stone

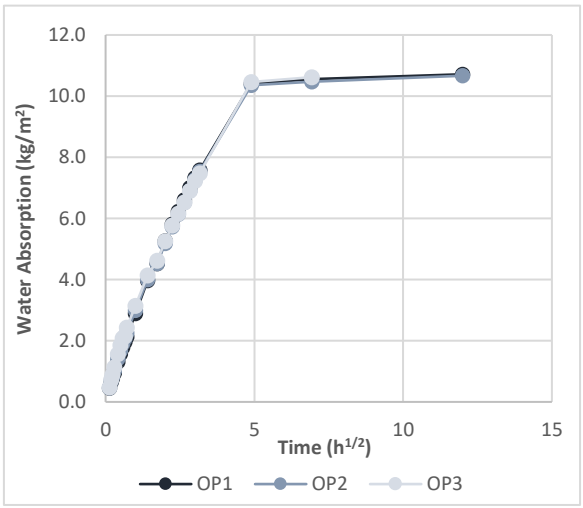

Graph 4: Capillary absorption - Opuka stone

Table 6: Capillary absorption coefficients of Božanov (BO), Mšene (MS) and Opuka (OP) stones

Capillary Absorption Coefficient ($kg/m^2 \cdot h^{1/2}$)				
Experimental Data				NAKI18* [23]
Sample	Individual	Avg.	SD	
BO-1	1.85	4.15	3.12	10.54 ± 2.01
BO-2	2.89			
BO-3	7.70			
MS-1	60.75	58.26	2.26	54.82 ± 8.42
MS-2	56.34			
MS-3	57.68			
OP-1	2.23	2.20	0.03	1.60 ± 0.03
OP-2	2.19			
OP-3	2.17			

***ČSN EN 1925: (2/2000) standard was used to determine the coefficients**

Figure 14: Aspect of Božanov stone during the capillary test revealing the heterogeneity of the stone as seen from the tortuosity of the wet front.

samples, the difference in the absorption coefficients is noticeable, but the difference in the maximum absorption capacities is more significant. These results suggest Mšene and Božanov are more heterogeneous than Opuka stone.

4.1.4 Drying at 50% RH

Graph 5 to Graph 7 depict the drying behaviour of the three stone types at 50% RH and at room temperature. Mšeno stone has the fasted drying rate, requiring approximately 8 days to reach a residual humidity of ca. 12.6%. Božanov takes almost twice of the time to dry, but reaches a much lower moisture content of ca. 2.9% after more than 16 days of drying. Finally, Opuka stone takes the longest period to dry requiring over 29 days to reach an average residual moisture content of 9.6%, placing it between the two types of sandstone in terms of moisture retention.

The results of this test are important as they more realistically show the drying process for masonry in-situ. Under the environmental conditions set in this experiment, Mšene, the stone with the fastest drying rate, can take over 4 days to lose a sufficient amount (ca. 80%) of its initial moisture content, which is considered a threshold to constrain capillary movement of water (and salt).

4.1.5 Drying at 50% RH with salt contaminated samples

To study the effect of salt on the drying behaviour of the stones, the drying test was conducted in the same specimens but after saturation with 14 w.t. % $Na_2SO_4 \cdot 10H_2O$ instead of distilled water. The drying curves are presented in Graph 8 - Graph 10.

As expected from the hygroscopic properties of sodium sulphate, the drying rate was reduced in most of the samples. Throughout the drying test the development of salt efflorescences was observed on all of the samples. In Božanov, the effloresce formed was characterized by a powdery layer covering the

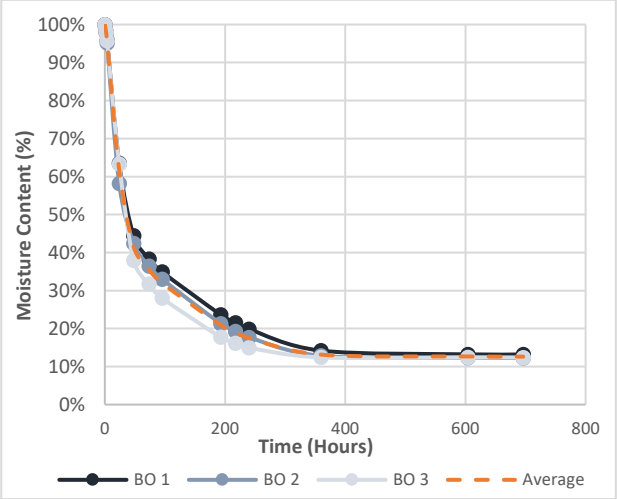

Graph 5: Božanov drying curve (water)

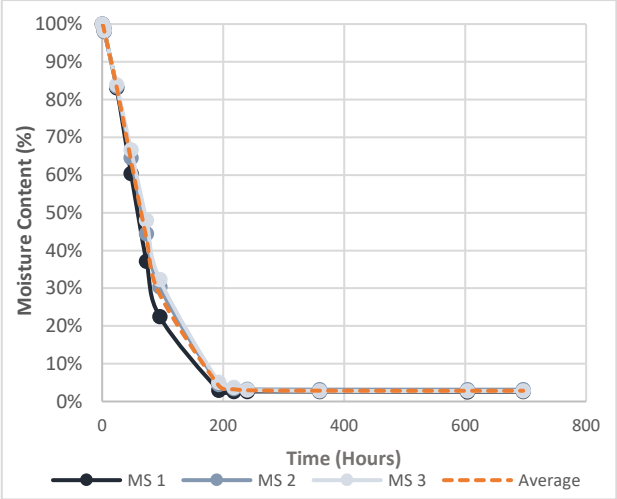

Graph 6: Mšene drying curve (water)

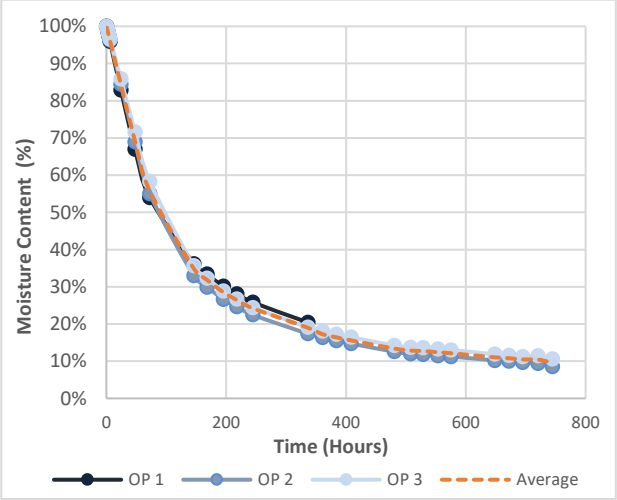

Graph 7: Opuka drying curve (water)

entire surface. In Mšene, a salt crust of ca. 5mm thickness formed. In the case of Opuka, two distinct types of crystal habits developed. On sample OP1 it took several days before any salt was macroscopically visible and the efflorescence ultimately formed had the aspect of a thin powdery crust. In stark contrast, samples OP2 and OP3 developed copious fluffy whisker-like salt efflorescences with ca. 10mm in height within the first 24 hours.

Graph 8 shows that the drying time for Božanov to reach its residual moisture content increased by more then 8 days when impregnated with salt. More significantly, is the more than double increment of the drying time for Mšene (Graph 9), taking approximately another 13 days to reach its residual moisture content. Further at 11.6%, the residual moisture content for Božanov has increased compared to water drying. In comparison Mšene's residual moisture content decreased to 6.7% when slat laden.

The results for Opuka (Graph 10) were a bit more varied as two of the samples (OP2 and OP3) were added to the drying test box at a later date. An unexpected increase in the RH of the testing box up to 60% was reached before the conditions were corrected. Possibly due to this RH variation, specimens OP2 and OP3 showed a different drying behaviour in respect to OP1. The increment in RH is also the most probable cause of different types of salt efflorescences developed, as previously described. The drying rate of OP 2 and 3 was faster when salt laden. The fluffy needle like efflorescence increases the specific area available for evaporation, which caused the rapid drying in OP 2 and 3 [36]. However, for sample OP 1, the drying speed was

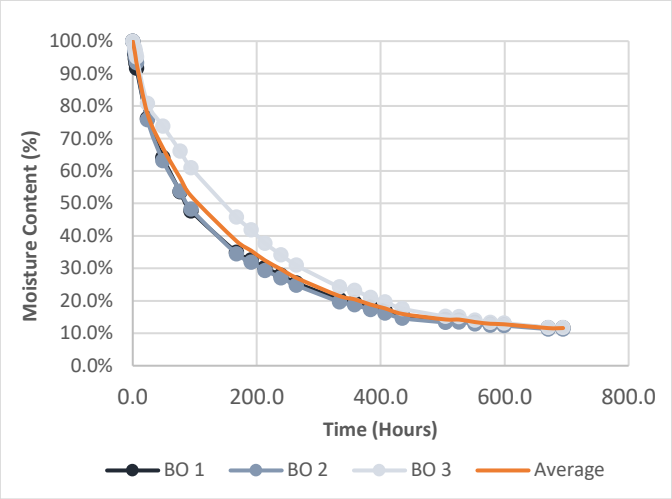

Graph 8: Božanov drying curve (salt laden)

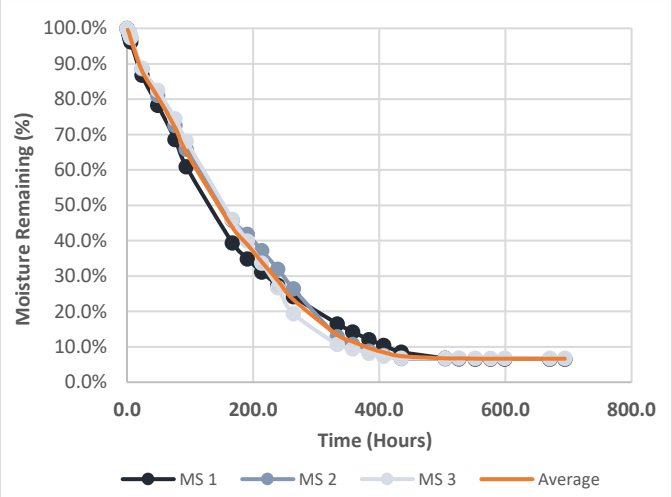

Graph 10: Mšene drying curve (salt laden)

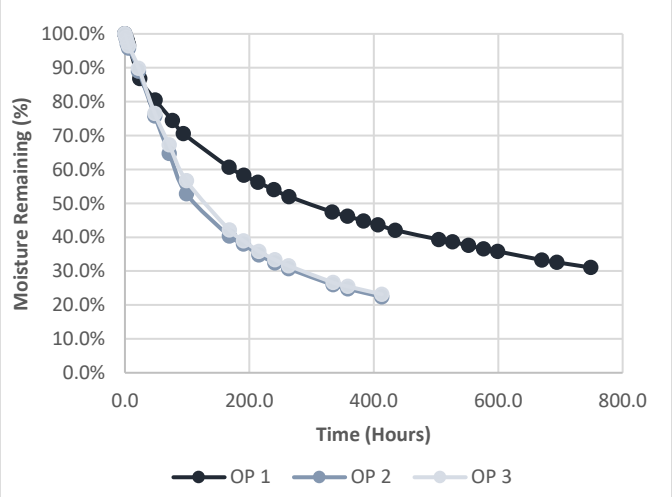

Graph 9 : Opuka drying curve (salt laden)

approximately the same suggesting the influence of salt within Opuka has less of a negative effect on drying compared to the other stone types.

4.1.1Drying Speed

The drying speed of Božanov and Mšeno was tested to ensure that the selected time for drying at lower temperature in the new aging test would be sufficient to eliminate most of the water introduced (>80%). As Opuka was added to the experiment after the procedure had been set, it's drying speed was not analyzed in the same manner. The specimens were wetted for 2h by immersion in water.

After the initial two hours of drying at 60˚C both stone types had already lost at least 80% of the water introduced. At 40 ˚C the Božanov stones had lost more than 60% of the water content, but the Mšeno ranged from 50-69%. The next day all the stones were considered dry, as their water loss ranged from 97-100%.

This quick test also allowed estimating how much salt solution each type of stone would absorb during the 2h-wetting phase of the ageing tests. On average, the Božanov stones absorbed 4.36% water while Mšeno absorbed 10.44%.

4.2 Accelerated Salt Crystallization Aging Test

4.2.1 General Observations

Throughout the aging cycles visual observations were made to track the changes in the degradation of the visual appearance of the specimens. A summary of the changes, trends, and anomalies observed over the 12 salt crystallization cycles follows.

Božanov

In general, Božanov showed little alterations to its initial visual aspect. A comparison of the stones from their sound state and after 12 wet/dry cycles is presented in Figure 16, which demonstrates that the overall size, shape, and colour was not significantly affected. Some erosion and rounding of the edges was noticed, however the most notable visual change was on specimens subjected to Test Procedures 3 and 5 in which the contamination was achieved through partial immersion. On these specimens, a film of white salt efflorescences was observed after drying. During the wetting phase, this 'film' of salt was observed as well. It was first noticed not by visual observation, but by touch; the texture of the surfaces felt 'slimy' when they were removed from the immersion dish. As more cycles were performed, the 'slimy' layer continued to build up until it was visible in both wet and dry states. This layer likely formed on the sides where the evaporation flux was strongest during the wetting phase. Comparing the samples from procedures 3 and 5, this crust was more significant on the specimens used in Test Procedure 3, in which 14% sodium sulfate solution was used. For both reference specimens, no visual alterations were observed.

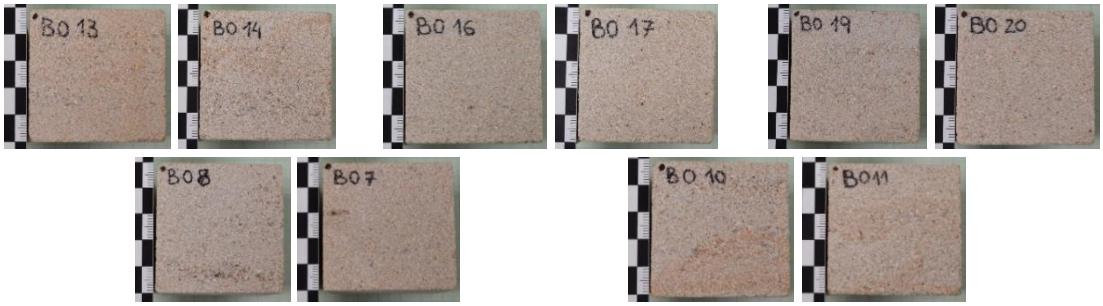

Before Aging

After Aging

Figure 15: Comparison of Božanov before and after salt aging cycles

Congruent with the insignificant change in the visual appearance of the samples, little to no loss of material was observed neither in the wet nor drying phase of each cycle. Small amounts of white fine sized particles (in the order of micrometers), were observed in the bottom of the immersion containers after some cycles. Large quantities of efflorescence were never observed after (or during) the drying stage. Most of the efflorescence formed was noticed within the first few cycles, when some small crystals were observed attached to the surface. As efflorescence crystallizes outside the specimen it does not contribute to induce damage.

Mšene

Of the three types of stone, the visual aspect of Mšene samples changed the most over the course of the salt aging cycles. In general, sand disintegration or sugaring was the main degradation pattern responsible for loss of material during ageing leading to the recession of the surfaces and to the rounding of the specimens' edges (Figure 17). Mšene samples also lost some material during handling. The samples that were subjected to salt contamination by immersion (i.e. Test Procedures 1, 2, and 4) showed the highest level of erosion of the edges. Samples contaminated with the highest salt solution concentration (i.e. Test Procedures 1 and 4) exhibited more severe deterioration. In general, a significant amount of material was lost during the wetting phase after the first ageing cycles. Between the two sets of specimens immersed in a 14 wt.% solution, those in Test Procedure 4, which were dried at a lower temperature, appeared to be slightly more damaged than those dried at high temperature. This aspect could be assigned to the fact that drying at a lower temperature facilitates the migration of salt towards the surface, thus increasing the level of damage within the superficial layers of the material.

Before Aging

After Aging

Figure 16: Comparison of Mšene before and after salt aging cycles

The specimens wetted through partial immersion also displayed material loss, although it was more concentrated on the bottom of the cube (i.e. where the evaporation flux was probably stronger during the wetting phase). Interestingly, this is in direct opposition to the results from Angeli, et al. [19] who reported that damage was stronger on the corners immerged in the salt solution. For samples subjected to Test Procedure 3, sandy particles of the stone were often dislodged from the evaporation surfaces during the wetting phase resulting in an uneven damage pattern (see Figure 18). Test Procedure 5 also induced this deterioration gradient increasing towards the evaporation face during wetting. However, the mass loss was lower. In the Test Procedures 3 and 5, material loss was more significant during the cycles when the stones were re-wetted with salt and sometimes the first following cycle with water rewetting. Similarly, to the observations done for the Božanov stone, no visual deterioration was detected in the Mšene reference samples.

The samples from all of the test procedures did not show any sings of efflorescences through out the aging cycles.

Figure 17: Mšene Test 3 (partial immersion) - heterogeneous deterioration

Opuka

Opuka exhibited a different pattern of visual alteration in respect to Božanov and Mšene sandstones. In all the testing procedures, the material losses were more important than those observed in Božanov, but the shape/visual aspect of the stones was not altered to the same degree as in Mšene. One significant difference observed after the first cycle was a slight colour change (darkening effect), which affected the whole surfaces in the samples used in Tests 1, 2 and 4 (complete immersion) and part of the side faces of the samples used in Tests 3 and 5 (partial immersion), i.e. up to which the salt solution front was registered, as shown in Figure 19. Opuka was the only stone type in which the salt solution (during the 2h-contamination phase) did not reach the top of the specimen from capillary rise from the bottom.

Figure 18: Colour change after one cycle with all test procedures in Opuka stone.

Being a much finer grained stone than the other two stone types, Opuka exhibited material loss as a fine powder. During the wetting phase, the release of material was not always observed until the samples were removed from the wetting container/dish. During such operations, a layer of very small particles would dislodge from the samples surface often making the contamination solution murky. The samples used in Tests Procedures 3 and 5 (partial immersion) didn't lose as much material as in the tests performed by total immersed. In these tests, a dusty layer developed on the evaporation faces of the stones up to the height reached by the salt solution front. In the samples contaminated via partial immersion lines of varying colour/shade resembling Liesegang patterns developed up to the height reached by the salt solution. The most significant material loss observed in Opuka occurred during the fourth cycle on sample 6 (Test Procedure 1). Figure 20, shows the large scale of stone which detached from the sample. This type of deterioration was only observed in one specimen and was assigned to a pre-existing crack that could be observed prior to starting the aging cycles.

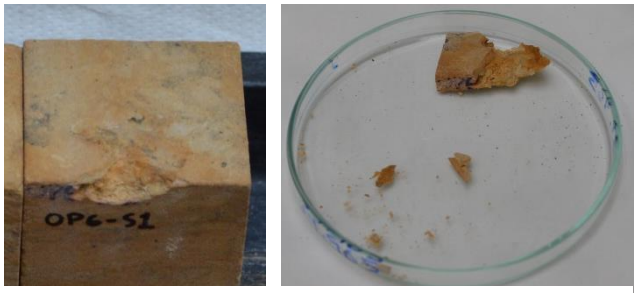

Figure 19: Opuka Test 1 Sample 6 - significant mass loss in cycle 4

4.2.2 Mass Evolution and Material Loss

As the contamination cycles progressed mass loss began to be easily noticeable in the Mšene samples, and to a lesser degree in Opuka and Božanov. Losses largely occurred during the wetting cycle, although the observation of mass loss was also seen during the drying stage, however it was often partially a result of handling. Even when handled carefully, sandy particles from the Mšene stones would often detaches even if touched lightly. Opuka samples would often have a light layer of dusty particles that would also come off when handled. As previously mentioned in the Methodology section, any large losses of material while handling the samples between the experimental stages was collected and weighted. However, within in each cycle the mass losses from general handling where very minute and therefore neglected.

From the recorded dry weights and the measured mass losses, trends in mass change of the three different types of stone and due to the five different testing procedures can be seen. For each of the tests, the average normalized mass variation and respective standard deviation (SD) is presented in Figure 20. In [4] three stages of the evolution of mass were defined as follows:

- Stage 1 – weight increase due to salt uptake.
- Stage 2 – positive or negative weight variation depending on competition between mass loss and salt uptake; begins after first visual damage (this stage may be non-existent).
- Stage 3 – weight decrease; salt uptake becomes negligible compared to stone damage.

In general, Božanov samples did not exhibit significant, if any negative, mass variation indicating their deterioration had not progressed beyond Stage 1. Furthermore, the standard deviation for the three

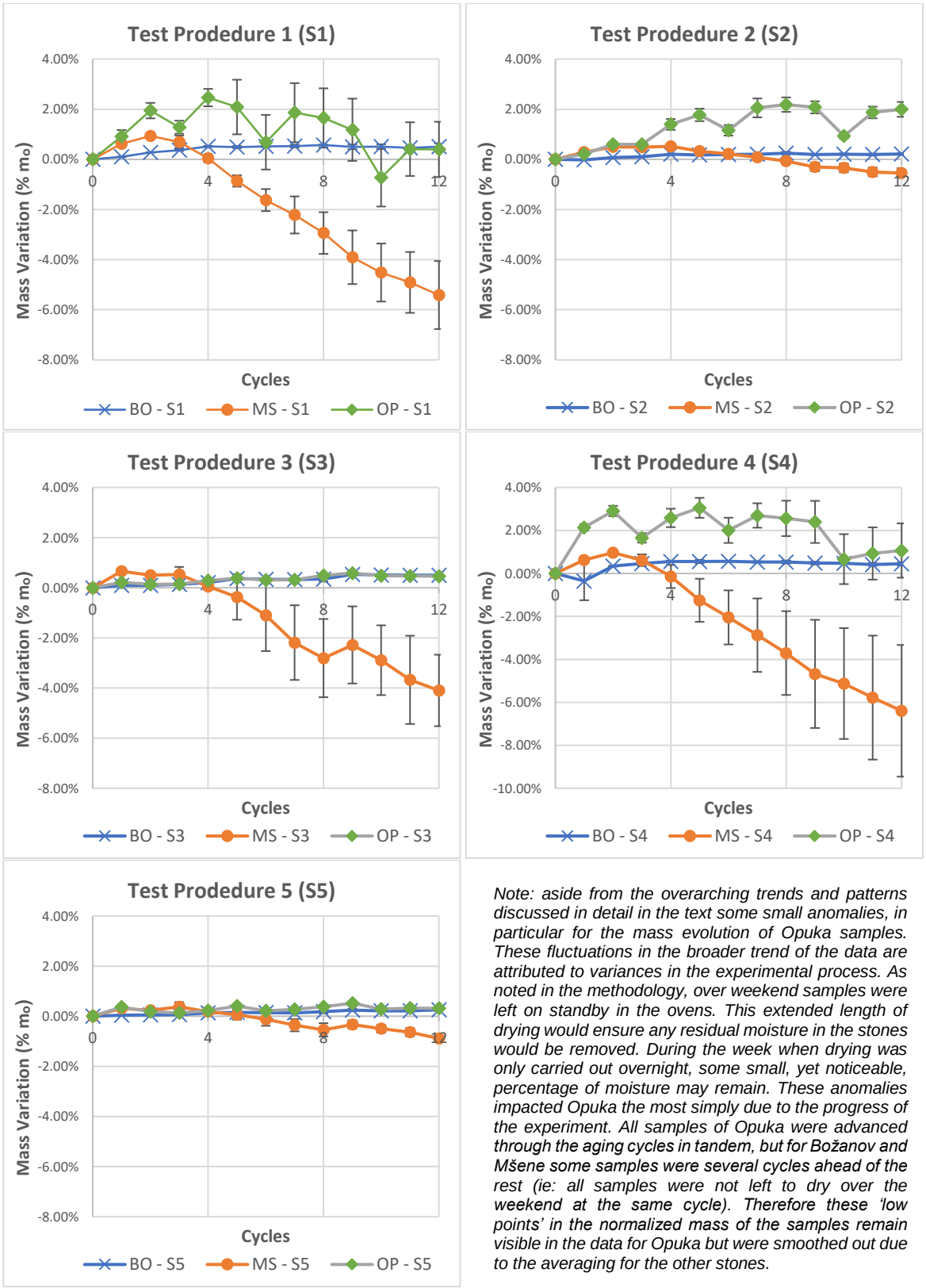

Note: aside from the overarching trends and patterns discussed in detail in the text some small anomalies, in particular for the mass evolution of Opuka samples. These fluctuations in the broader trend of the data are attributed to variances in the experimental process. As noted in the methodology, over weekend samples were left on standby in the ovens. This extended length of drying would ensure any residual moisture in the stones would be removed. During the week when drying was only carried out overnight, some small, yet noticeable, percentage of moisture may remain. These anomalies impacted Opuka the most simply due to the progress of the experiment. All samples of Opuka were advanced through the aging cycles in tandem, but for Božanov and Mšene some samples were several cycles ahead of the rest (ie: all samples were not left to dry over the weekend at the same cycle). Therefore these 'low points' in the normalized mass of the samples remain visible in the data for Opuka but were smoothed out due to the averaging for the other stones.

Figure 20: Normalized average mass variation for each type of test procedure (one SD shown)

stones in each test was very low. Mšene samples showed a short period of mass increase (Stage 1) followed by relatively quick mass loss causing the mass evolution to move directly into Stage 3. In the test procedures where the mass evolution began to decrease rapidly once entering Stage 3, the standard deviations became more significant. Opuka's behaviour was similar to Božanov's, although some tests induced enough damage in Opuka for the mass variation to reach Stage 2. Additionally, the standard deviation for Opuka reflects the heterogeneity of the stone as their rate of deterioration expressed by mass variation was more distinct between specimens used in the same test procedure.

Figure 21 presents the data of the collected and weighted material lost from each sample at 4 cycle intervals to distinguish the increase in a sample's mass due to salt uptake and decrease due to mass loss. The accuracy of the material loss values is obviously compromised by the small amounts of material lost during handling, which were not collected. From Figure 21, it is quickly observed that overall the most mass loss occurs in cycles 5-8 for all tests and stones types. This is believed to be partially due to the increased vulnerability of corners and edges to salt crystallization. These areas are subjected to evaporation from more than one side, increasing the salt concentration in these areas during drying. Therefore, supersaturation during wetting will be reached quickly (cycles 4-8), inducing damage. As the edges of the stones are rounded out, a more uniform salt gradient during drying will be formed, causing less supersaturation and in turn less damage (cycles 9-12).

When comparing the mass loss results of the different test procedures in each stone (Figure 20) it can be seen that the results of Tests 1 and 4, performed at high and low drying temperature, respectively, are very similar. Regarding Mšene samples, the decrease in mass variation (Figure 20) is slightly higher in Test 4 than in comparison with Test 1, which is in line with the percentage of mass loss (Figure 21) and with the visual observations described previously. However, the standard deviation is also higher in Test 4. The lower temperature provides a slower drying rate by enabling capillary transport during drying for a longer time. As the kinetics of evaporative drying draws the salt towards the surface of evaporation, higher accumulation of salt can develop in the outer layer of the stone. Hence, in the following wetting phase, the conditions for reaching supersaturation (and damage) are favoured in this layer. At the high drying temperature employed in Test 1 (EN 12370), the critical moisture content limiting capillary transport is reached more rapidly, thus preventing salt supply to the surface. Using a lower drying temperature seems to increase the deterioration at the surface, which is the common situation in natural exposure conditions. However, given the high standard deviation in Test 4 and the relatively small difference in mass change between the two tests, further tests (and with a higher number of specimens) are required to confirm the effectiveness in obtaining surface damage by drying at a lower temperature. Although Test Procedure 5 was also dried at the lower temperature, it is difficult to draw any conclusions from its mass loss data infer about the effect of drying at a lower temperature. Test 3 is the most comparable procedure to Test 5 regarding the contamination procedure, i.e. wetting by partial immersion and re-wetting with water. However, a higher drying temperature and a greater concentration of salt solution were used in Test Procedure 3. Due the very minimal deterioration seen in all the samples

subjected to Test 5 after 12 cycles, and the lack of definite discrepancy due to the change in drying temperature between Test 1 and 4, it is believed that the impact of the change in salt concentration overshadows the effect of the drying temperature.

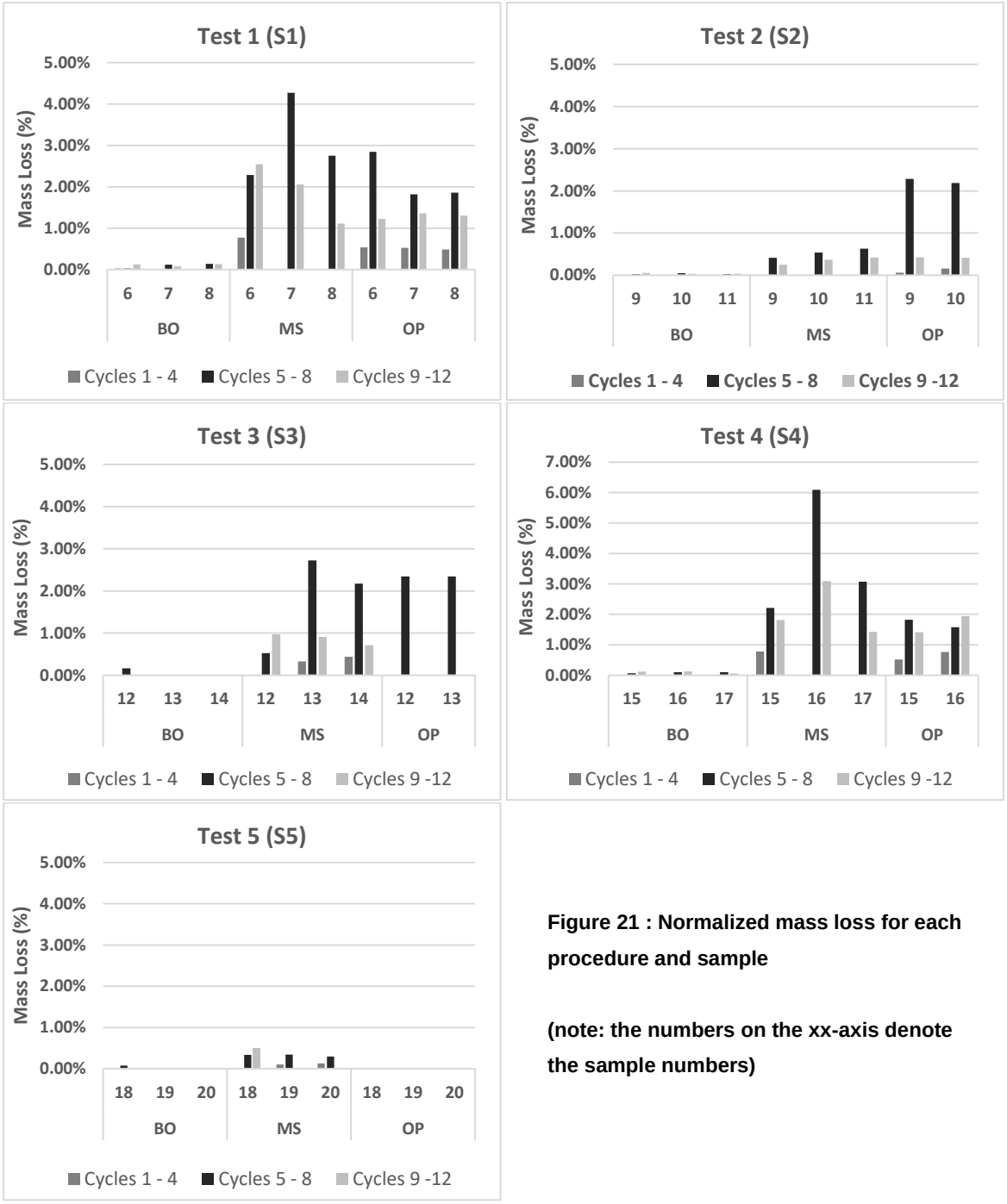

Figure 21 : Normalized mass loss for each procedure and sample

(note: the numbers on the xx-axis denote the sample numbers)

Regarding the effect of the salt solution concentration on the mass variation, the impact is clear when comparing the results of Tests 1 and 2, and Tests 3, 4 and 5. There is a remarkable difference in the evolution and overall mass change seen in the graphs of Figure 20. The average mass deviation of Mšene samples in Test Procedure 1 decreased down to -5.4% in Cycle 12, whereas in Test 2, the net

decrease didn't even reach an average of -0.6%. Furthermore, the mass loss data shown in Figure 21 confirm that a higher percentage of material was lost in Mšene and Opuka stones in Tests 1 and 2. Additionally, the average mass deviation for Opuka in Test Procedure 1 had begun to decrease more by the end of the 12 cycles, indicating that the samples were likely starting to begin Stage 3. However, in Test 2 the trend had leveled down to ca. 2% indicating that the samples were still in the second stage of deterioration where salt uptake and mass loss are at odds. As discussed in the State-of-the-Art section, the most important factor inducing damage with sodium sulfate is achieving supersaturation during the wetting phase [3]. For samples contaminated with 14wt.% versus 7wt% salt solution concentration, there is twice as much salt available when using 14 wt.% resulting in a more rapid pore filling. In Tests 1 and 4 (using 14 wt.% solution, the maximum weight increment occurs up to Cycle 3, after which the decrease in mass would indicates that the porous network has been filled with salt up to a threshold value allowing for supersaturation to occur in the pores during the following wetting phases.

In respect to Test 2, the maximum mass increment is lower and is reached one cycle later (Cycle 4). This combined with the much slower rate of mass decrease afterwards suggests less crystallization pressure is being induced. Regarding Test Procedures 3 and 5, where concentrations of 14wt.% and 7wt.% solution were used respectively, the mass evolutions for Božanov and Opuka are not significantly different, but a clear increment in damage can be seen for Mšene in Test Procedure 3. Mass loss in Figure 21 shows that more damage is caused in Test 3, as cumulatively no samples subjected to Test 5 lost even 1% of its initial mass. In previous studies [37] [1], several authors reported that increasing the sodium sulfate solution concentration lead to higher damage at a faster rate.

Considering the amount of lost mass collected from samples in Tests 1 and 2, most specimens appear to have lost more material during Cycles 5-8 versus Cycles 9-12. With respect to Mšene samples that showed the highest level of deterioration, as mentioned before it can be argued that after the more vulnerable edges and corners of the samples were rounded off, less material was subsequently lost because salt had to accumulate in the stone body to produce enough crystallization pressure to damage the less vulnerable mass of the samples. In Opuka, the edges were not as much affected, so the geometric vulnerability could not explain why less material was lost in cycles 9-12 then in 5-8, particularly in the Tests 2 and 3. Two possible explanations for this behaviour are experimental error (not enough cooling time after drying to return the samples to room temperature before wetting again), or possibly too much handling during cycles 5-9, causing more material to be dislodged. Further cycles could help clarify these trends. Compared to other studies that carried out up to 15-60 cycles [12] [38] and the lack of complete disintegration of any of the specimens in this research it is felt additional cycles are required to better understand how sodium sulfate crystallization would continue to affect the deterioration patterns of the stones.

Finally, the difference between Tests using partial immersion and re-wetting with water, compared with complete immersion and re-wetting with salt solution are considered. As discussed in the Visual Observation section, from the beginning, differences in damage locations for the three stone types can

be distinguished between partial and complete immersion samples. Looking at the graphs of mass variation (Figure 20) and mass loss (Figure 21), the deterioration in Božanov is very small showing no distinctive differences between Test procedures. Significant differences can be seen in the behaviour of Opuka and Mšene, which have very different capillary absorption coefficients (See section 4.1.3).

Opuka has a low capillary absorption coefficient, which is reflected in the fact that in Tests 3 and 5 (partial immersion), the salt solution (and water) during the wetting phase, never reached the top of the specimens. Less salt solution absorption combined with re-wetting with water explains why the mass increase in Test 3 is much lower than in Tests 1 and 4, where complete immersion was used during the wetting phase and more salt was supplied in each cycle. The notable reduction of salt content in samples used in Test 3 is also evident in comparison with the mass evolution in Tests 1 and 4 for Opuka appear to be starting to decrease, shifting into the third stage of deterioration where mas loss dominated over salt uptake. However, the mass variance in Test 3 is relatively constant while the mass is lower, thus indicating that a critical content of sodium sulfate enough to induce damage has not been reached.

In contrast to Opuka, Mšene has a high capillary coefficient, so when the wetting phase was performed by partial immersion the capillary moisture content (i.e. the amount of water or salt solution absorbed by the sample sufficient to wet the upper surface by capillary rise from the bottom) was reached within only one minute. This behaviour explains why in the first cycle of Test 3, in which the specimens are wetted with the 14wt.% salt solution, they absorbed a similar amount of salt as those subjected to immersion in Tests 1 and 4 (Figure 20). In the following cycles, where re-wetting is done with water, the mass decreases, possibly due to the fact that some salt is washed out from the sample upon contact with water in the immersion dish. However, as it is evident form the mass loss values of Mšene samples in Test 3 and the overall negative trend in mass variation towards the end of the cyclic testing, the contamination with salt in Cycles 1, 5, and 9 did introduce a sufficient quantity of sodium sulfate to induce material loss. However, specimens in Tests 1 and 4, in which salt solution was used in every wetting phase, the overall mass loss was higher (Figure 21).

Comparing Test 2 (total immersion) with Test 5 (partial immersion), in which a 7wt.% solution was used, similar trends in mass variation as described for Mšene were registered, but to the variation was less significant, probably because a lower salt solution concentration was employed. Furthermore, the degree of damage expressed as mass loss is also lower in these procedures.

In summary, the salt solution concentration seems to have had the most significant impact on the degradation degree of the stones. The evolution of mass for Tests 1, 3, and 4, in which a 14wt.% salt solution was used, demonstrate the most negative variation. Generally, the highest percentage of lost mass was collected form these three tests. The influence of changing the drying temperature may have an influence on the degree of deterioration, however more tests and samples are required to make sound conclusions. The impact of contaminating samples via complete or partial immersion appears to depend more on the absorption properties of the materials than on the procedure its self. Contaminating

the samples with salt solution every few cycles and re-wetting with water in-between reduces the deterioration process.

4.2.3 Ultrasonic Pulse Velocity (UPV)

In their sound state prior to commencing the salt aging cycles, Opuka exhibited the fastest velocity followed by Božanov and then Mšene (Table 8). Over the course of the aging cycles the decrease in velocity is in general the greatest for Opuka, then Božanov and Mšene again. However, despite the greater decrease in velocity of Opuka and Božanov samples, the relative order of fastest to slowest velocity doesn't change at the intervals of 4, 8, 12, and post desalination when the ultrasonic velocity was tested.

Table 7: UPV average from five readings per stone in sound state

Average Velocity (mm/µs)			
Procedure	**BO**	**MS**	**OP**
Test 1	2.71	1.80	3.39
Test 2	2.94	2.08	3.42
Test 3	2.97	2.05	3.46
Test 4	3.04	1.77	3.64
Test 5	2.87	1.93	3.40

In Graph 11 to Graph 13 the UPV is presented for each stone type and test procedure. For relative comparison, the velocities were normalized with respect to their velocities in the undamaged state. The broad trend seen is a significant decrease in velocity after 4 cycles, followed by a small or possibly no significant change between cycles 4 and 8. After 12 cycles, there is a definite increase in the velocity, bringing many of the stone layers to a velocity greater than even their original reading in the sound state. This occurred more for Mšene and Božanov samples, while the velocity of Opuka samples mostly increased to approximately their sound velocities or a little slower. Finally, after desalination ('washed'), most samples demonstrated a drop-in velocity again.

As previously discussed, the value of UPV is affected by physical and mechanical properties, most notable for this discussion are aspects such as porosity, pore size, and microcracks [5] [22]. The initial decrease in velocity seen across all the tests and samples could be from the start of damage and alteration to the porous network due to salt crystallization. The subsequent small increase or plateau between cycles 4 and 8 might be from the detrimental effect of damage from the salt crystallization competing with the positive effect of pores filling with salt. The authors Rossi-Manaresi and Tucci posit that salt can have a cementing or consolidating effect if the crystallization pressure is still below the materials mechanical strength and this can cause the UPV to increase [39]. Additionally, decay at this stage in the aging process was loss of mass from the edges, and faces of the samples, especially for Mšene. Perhaps, these vulnerable surfaces were suffering the damaging effect of the salt crystallization cycles. However, the overall porous network of the stones was not being further altered (i.e. increase in pore size, or development of microcrack). As salt continues to fill in the pores of the stones, this cementing behaviour has an increasing effect, to the point where the UPV measurement after 12 cycles is much closer to the sound state velocity. After desalination, the salt and its positive consolidating effect are removed so the ultrasonic velocities decrease again.

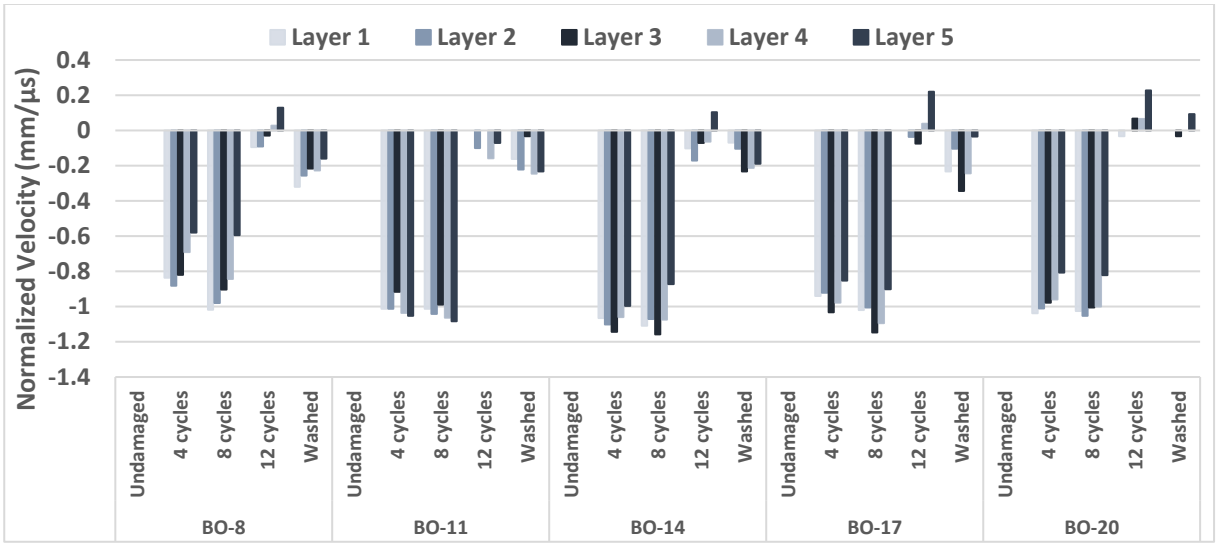

Graph 11: Normalized ultrasound velocity for Božanov samples

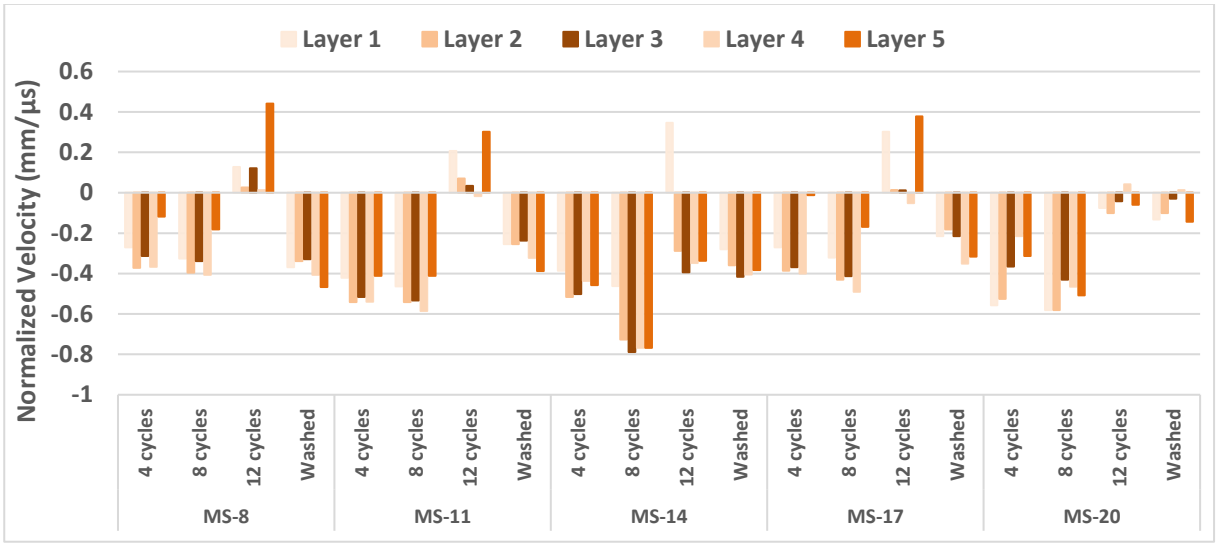

Graph 12: Normalized ultrasound velocity for Mšene samples

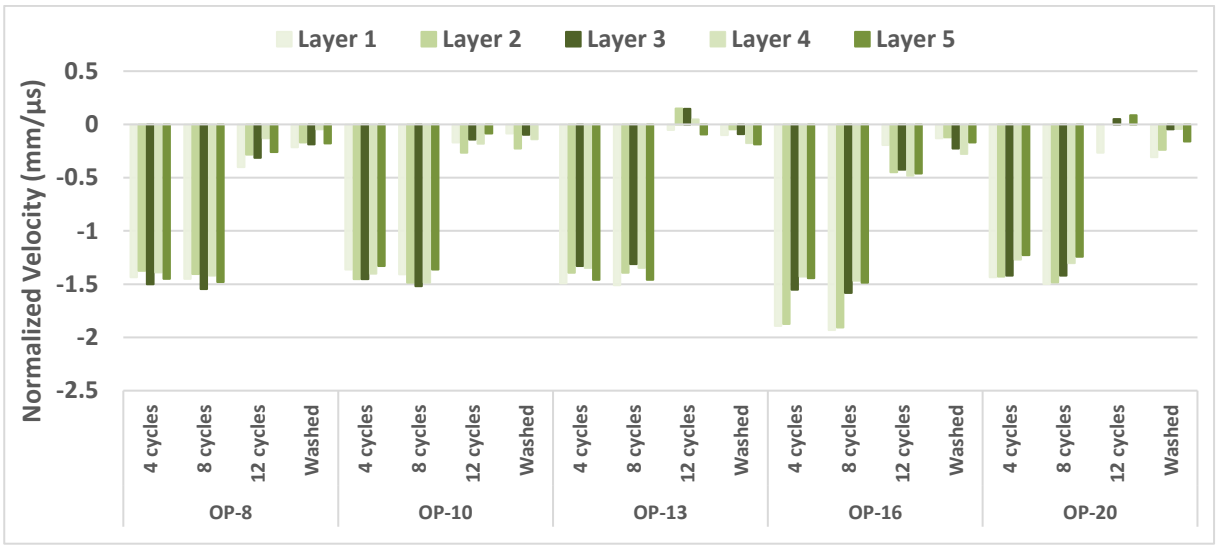

Graph 13: Normalized ultrasound velocity for Opuka samples

On first glance, this general process seems plausible, however on further comparison between the results seen in the different test procedures and between the three stone types, there remain a number of inconsistencies. Further, the patterns of deterioration, and the relative decay noted in the two preceding sections (4.2.1 General Observations and 4.2.2 Mass Variance and Material Loss) with respect to the variations in the testing procedures and the characteristic of the stone are not reflected in the UPV data.

Mšene exhibited the highest mass loss, however the samples have the smallest variations in UPV. In general test procedures that used 14wt.% solution (Tests 1, 3, and 4), and those that employed complete immersion with salt solution re-wetting (Tests 1, 2, and 4) showed more damage. However, from Graph 11 one can see that the samples of Božanov show close decreases in velocity after 4, and 8 cycles, however sample BO-14 subjected to Test 3 demonstrated the greatest decrease while sample BO-8 (Test 1) shows the lowest change in UPV. This same phenomenon is seen within the samples of Mšene (Graph 12) and is even more pronounced with the sample from Test 3 (MS14) showing -0.1 to -0.3 mm/us more decrease in velocity the sample from Test 1 (MS8). For Opuka, sample OP16 from test 4 has the greatest velocity decrease, yet Test 4 used 7wt.% solution. Even within the different layers of each sample so striking patterns are seen. Some consistency in the relative ranking of velocity between the layers is seen at each stage (i.e. after 4 cycles, 8 cycles, etc.). However, one might expect to see a pattern in the samples contaminated via partial immersion (Tests 3 and 5) compared to the tests with complete immersion (Tests 1, 2, and 4), yet after 4, 8, and 12 cycles, there are still no clear pattern. Possibly the natural heterogeneities of the stones are outweighing the impact of the salt distribution and internal damage within the stones. Alternatively, perhaps there were errors in the testing procedure that resulted in the discrepancies seen in the data.

As discussed previously, ultrasonic velocity can be affected by a number of factors (e.g. porosity, density, weathering, moisture content [22]). As referenced in Ahmad et al. literature review on ultrasonic testing [22], “Durrast et al. showed that the decrease in ultrasonic pulse velocity due to deterioration cannot be accurately explained based only on porosity increase but changes in stone fabric also have to be taken into account”. It is possible that there are trend and important observation within the data, but are being obscured by too many changing factors within the testing procedures and the small difference in each sample physical properties. Furthermore, the deterioration of the faces of the specimens would also cause a reduction in the UPV path which was not accounted for, and an increase in the unevenness of the contact surface for the equipment which may have also introduced error.

4.2.4 Salt Distribution

The concentration and distribution of sodium sulfate throughout the stones was analysed to better understand the impact of the changed parameters on salt crystallization. Due to limited time, and as mentioned in the Methodology section, only a selection of the aged stones was tested. Stones of all three types were analysed for Test Procedures 1, 4, and 5. These procedures were selected as 1 & 5 encompass all the differences in parameters explored. Additionally, 4 follows EN12370 with the

exception of the drying temperatures. Bases on the conductivity curve that was developed (Appendix A), an approximate concentration of salt within each layer of the stone was calculated and is shown in Graph 14.

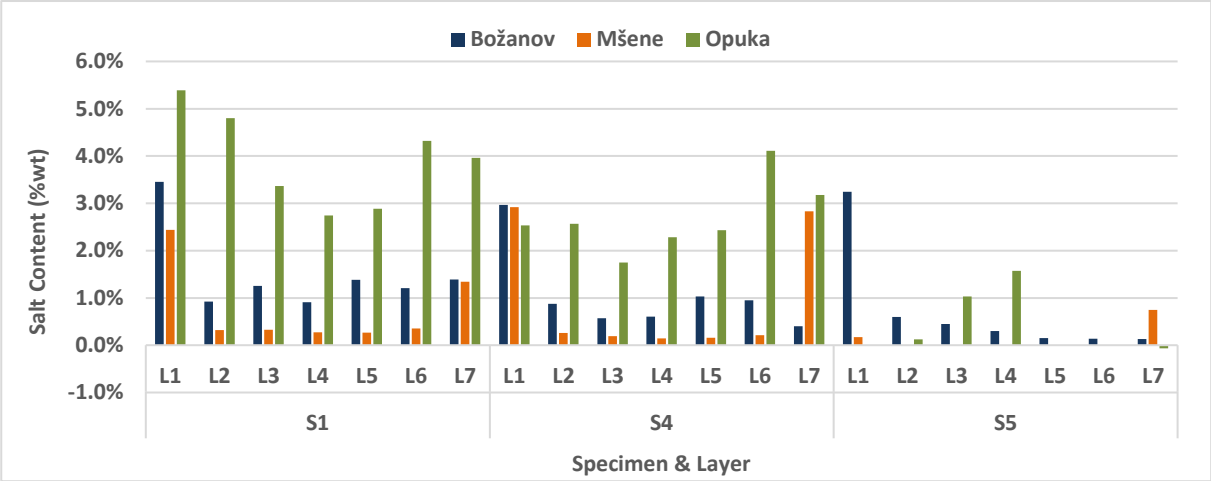

Graph 14: Salt distribution comparison between three of the test procedures (L1-L7 denote the 'layer' the sample was extracted from, starting from the top of the specimen)

From analysis of the findings it can quickly be seen that the relative salt content for the samples from test 5 contain significantly less salt then their counterparts subjected to the other tests. However, given that 7wt% solution and rewetting with water is prescribed in this procedure this observation was expected.

It's interesting that across all three test procedures, Opuka on average shows a higher percentage of salt than Božanov and Mšene. This stands out as Opuka didn't show any intense signs of deterioration, nor were large concentrations of salt observed with SEM (discussed in section 4.2.5). The minerals and compounds that constitute the fabric of the stones can itself contribute ions, and therefore increase the conductivity of the solution. When small samples of the water aged specimens were also ground and mixed with water, it was found that Opuka stone increased the conductivity of the distilled water the most. Attempts were made to remove the influence of the stones conductivity, so the data presented in Graph 14 should only reflect only the salt content. Nevertheless, this observation is an outlier in the context of observations from other analysis techniques.

However, lets also consider the apparent salt content in the three specimens of Mšene. In contrast to Opuka, Mšene has the lowest salt content in general of the three stone types. Further, Mšene was observed to have the highest mass loss, and salt surface crusts were observed with SEM on almost all samples. The significantly higher salt content in layers 1 and 7 for Tests 1 and 4, are congruent with the idea of a salt accumulation close to the surface. However, the salt distribution findings still show that the stone with the least salt content (Mšene) experienced the most damage. If it is considered that the drying dynamics in Mšene deposit a large portion of the salt near the outer layer, then supersaturation would be easily achieved, inducing damage in the following wetting phase. Since most of the salt in Mšene is

transported to the surface during drying, and then subsequently dislodged during the next wetting phase, the lower concentration of Mšene is reasonable. Compared to Božanov and Opuka, Mšene has a lower mechanical strength, thus less crystallization pressure is required to inflict damage. Consequently, a higher accumulation of salt within the pores of Božanov and Opuka can occur, despite less damage observed compared to Mšene. These observations of greater salt content and less damage in Opuka versus Mšene suggests that the high mechanical strength of Opuka overcomes its susceptibility due to a small PSD.

Considering the salt distribution for the three Božanov specimens, the salt content in L1 (the top ca.5mm of the stone) is markedly higher than the other layer. The fact that the values for this exterior layer are higher than the interior layers is not unusual, because as discussed previously, the dynamics of the drying process would cause more salts to move towards the exterior faces. What is odd, is the fact that in L7, the bottom slice of the stone and therefore also the external face, does not show a similar content. In the Mšene and Opuka samples this behaviour of having more salt content in both outer layers is seen.

Božanov has the largest pores, and was the only specimen to develop visible efflorescence in the pores on the surface. Since the specimens were always placed with L7 downward, it's possible that these salt crystals in the surface pores of Božanov were dislodged during handling. This is one possible explanation for why the top layer of the Božanov samples rom Test 1 and 4 had a higher salt content then the bottom.

With respect to differences in the salt distribution seen between the test procedure that can be attributed to the changes experimental factor, definitive conclusions are hard to draw. When looking at the salt content of Opuka in Test 1 versus 4, in general there seems to be more salt in Test 1, suggesting the drying temperature affects the salt distribution. However, the same trend in not observed in Mšene and Božanov. The remarkably low salt content in almost all the samples from Test 5, indicate that the lower salt content, and rewetting with water prevents the accumulation of sodium sulfate in the stones.

4.2.5 Microstructural Analysis with SEM – EDS

Reference Procedure -Sample 5

In the general observations, it was noted that no decay was seen in the reference samples (i.e.: water aged) for any of the stone types. Nevertheless, samples of each were observed with SEM and a sample of the findings are presented in Figure 22. As was expected no sign of alteration were observed. Due to the lack of decay these samples give a baseline idea of what each of the stone types look like in the sound state. The texture of the two sandstones is significantly courser than Opuka as can be seen by comparing the SEM images of Mšene and Opuka in Figure 22. Both images are at the same magnification. Reflecting the petrographic and physical characteristic described for each stone in section 4.1.1, Opuka exhibits a fined grain matrix. Božanov and Mšene structure looks like conglomerates of sand particle aggregate. Figure 22 depicts the structure of Božanov's binder.

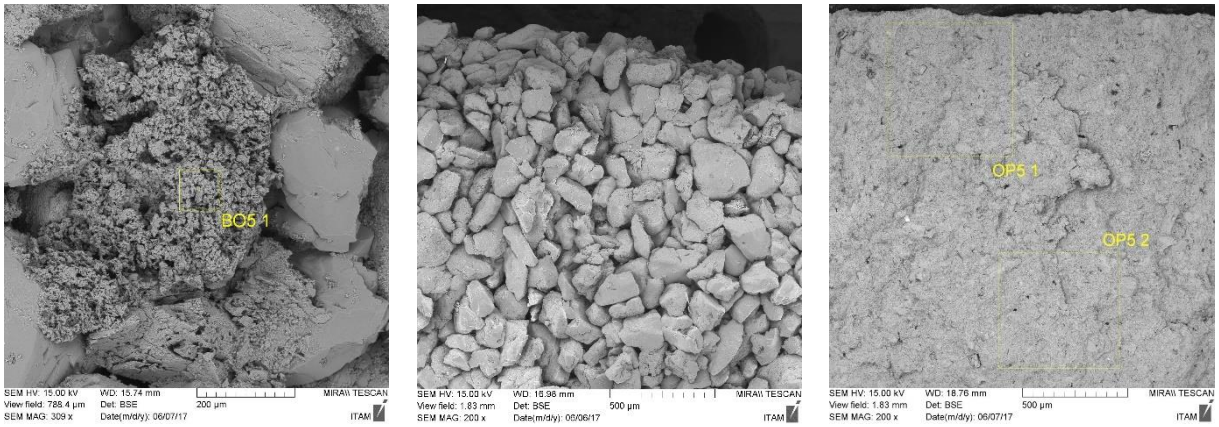

Figure 22: SEM investigation of reference (water aged) samples
Božanov binder (left), Mšene (center), Opuka (right)

Test Procedure 1 – Sample 6

Test procedure 1 which followed the EN12370 standard, used both the 14wt.% sodium sulfate solution and contamination via complete immersion in each cycle. Therefore, of all the samples, those in Test 1 are expected to have high salt content. Presented in Figure 24, MultiPoint area analysis of the samples collected from Božanov and Mšene stone show increased amounts of sodium sulfate within their porous network. In the sample BO6 the salt distribution is more uniform throughout, while MS6 the salt is concentrated in the first millimetre close to the exposed surface. Although the salt crystals are more difficult to distinguish without the aid of the elemental mapping for the Božanov sample, the surface crust on Mšene can be seen even in the overview image of the sample (Figure 24, middle row left image). These two types of salt distribution suggest different behaviours during drying. As was show in the capillary absorption test, both sandstones undoubtedly become fully wetted within the two-hour immersion phase. Therefore, the difference in salt distribution in believed to be due to salt transport mechanisms during drying. Since both samples were dried at the same temperature, the difference in the structure of the porous network must account for the difference response to salt aging. Mšene stone, has smaller pores than Božanov, but more importantly, it's porosity is notably larger; 29.7% compared to 17.4% (see section4.1.2.). A higher absorption capacity of Mšene in comparison to Božanov leads to a higher salt solution uptake. With more water in it's network, and a slower initial drying rate (Graph 8 versus Graph 9), Mšene stone will take longer to dry, allowing more time for the mechanics of capillary transport, driven by the evaporative drying at the specimen's surface, to draw the sodium sulfate closer to the surface to the edge of the stone.

In contrast to the large amount of salt seen in the two sandstones, salt was not readily found with area mapping on the sample of Opuka. Additionally, all three points where elemental mapping was done (location displayed in bottom left image of Figure 24) showed no accumulations of salt in pores. Opuka's porosity is between Mšene and Božanov, however it's absorption coefficient is significantly lower because the average pore size diameter is significantly lower. During the Capillary absorption test, even

after 8 hours, the water front has not reached the top of the sample. The reduced salt solution uptake could explain the lack of salt observed with SEM for Opuka, but in contrast the analysis of salt distribution (section 4.2.4) found that Opuka had the most salt content. The most likely situation is that there is salt in the pores of Opuka, but it was not detected by the elemental mapping. The surface of the SEM samples was very uneven, which can cause areas of the specimen to be unobservable. Furthermore, the size of Opuka's pore, which is significantly smaller than the two sandstones, means that salt crystals in the material would also be very small and spread throughout the material. Perhaps if the samplers were viewed with a greater magnification, the salt crystals could be found.

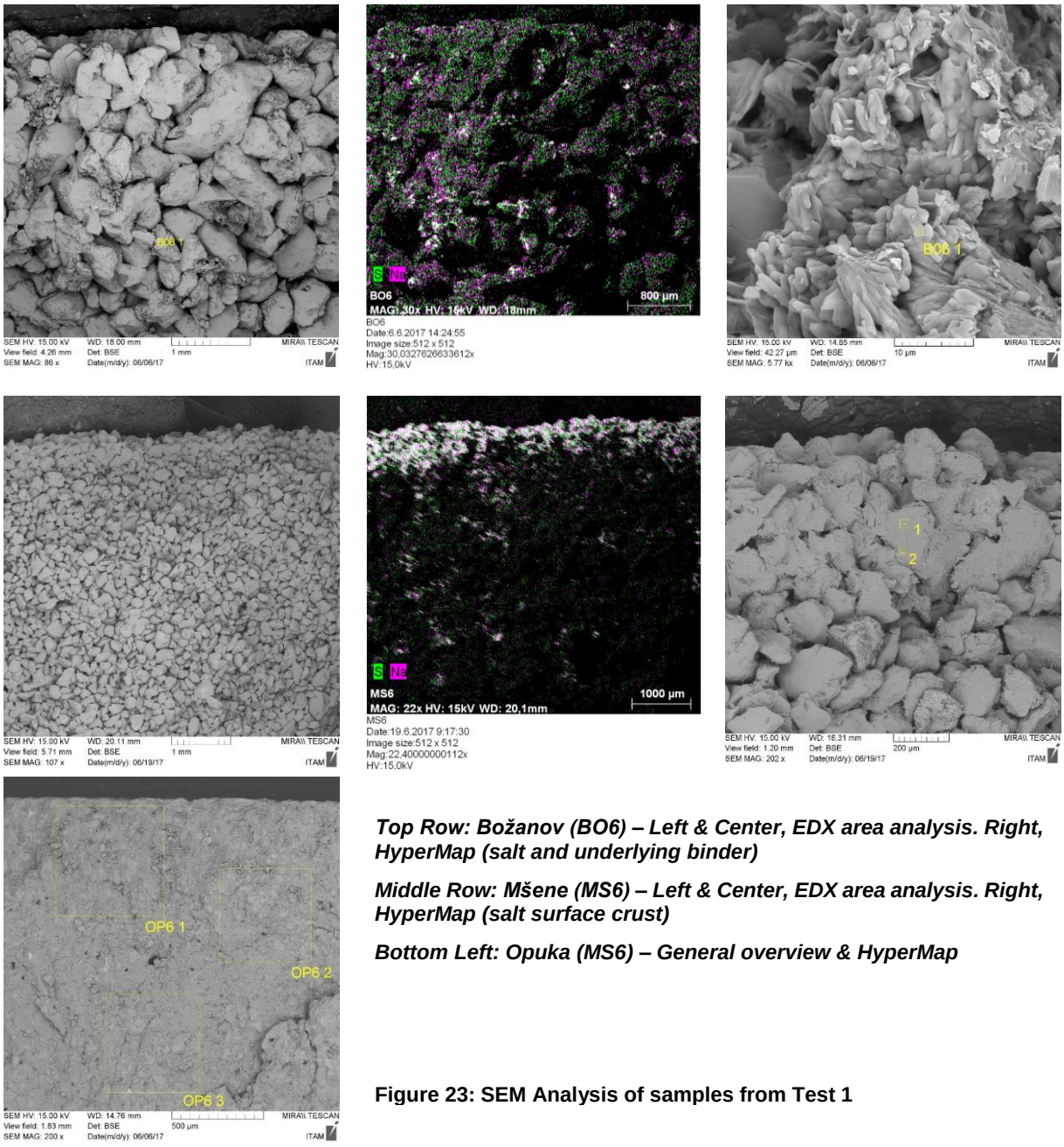

Top Row: Božanov (BO6) – Left & Center, EDX area analysis. Right, HyperMap (salt and underlying binder)

Middle Row: Mšene (MS6) – Left & Center, EDX area analysis. Right, HyperMap (salt surface crust)

Bottom Left: Opuka (MS6) – General overview & HyperMap

Figure 23: SEM Analysis of samples from Test 1

Test Procedure 2 – Sample 9

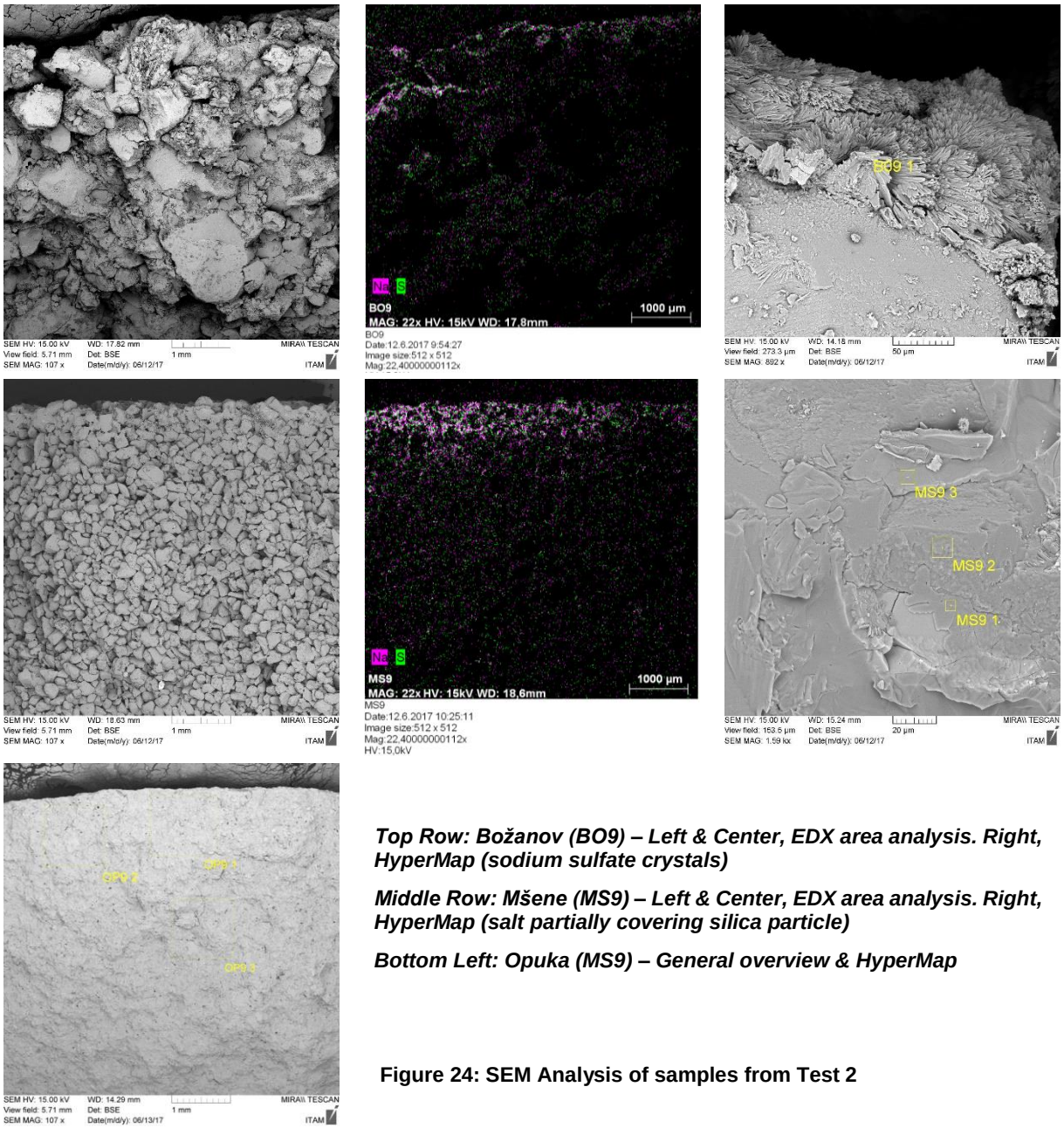

Top Row: Božanov (BO9) – Left & Center, EDX area analysis. Right, HyperMap (sodium sulfate crystals)

Middle Row: Mšene (MS9) – Left & Center, EDX area analysis. Right, HyperMap (salt partially covering silica particle)

Bottom Left: Opuka (MS9) – General overview & HyperMap

Figure 24: SEM Analysis of samples from Test 2

In Figure 25, the elemental mapping (HyperMaps) for the Božanov and Mšene samples show the development of a surface crust on both stones. This is the same salt distribution pattern as in Test 1 for Mšene, however not for Božanov. The SEM analysis conducted does not provide a quantitative measure of the salt observed, therefore it is hard to say if the quantity of salt distributed through the Božanov and Mšene samples is different than the results of the samples from Test 1 and 2. Nevertheless, the accumulation of salt close to the surface for Božanov in this test suggest the reduction in concentration of the salt solution impacted the amount of salt close to the stone surface. The lower salt concentration means a higher viscosity and therefore a higher capillary transport rate drawing salt to the surface

resulting in the visible concentration of salt at the surface [40]. Unfortunately, the entire cross-section of samples was not analysed to get a complete picture of the salt distribution. However, this type of analysis could be informative, and can be compared with salt distribution assessment from other methods (e.g. electrical; conductivity, or hygroscopic moisture content).

Also shown in Figure 25 are up-close images of salt crystals found in the pores of the two sandstones. The crystals found in BO9 show an elongated sub-angular shape (needle-like appearance) in contrast to the salt crust observed in MS9. It is hard to make any conclusions about the type of crystals that will form due to the stone type or test condition though, as the salt shown on a pore of BO6 in Figure 24 (top right image) has yet another distinct appearance to it.

Salt was also not found in the sample of Opuka from Test 2 (OP9). Once again, a MultiPoint analysis was done and three different points on the sample were analysed with elemental mapping, however same as the analysis of OP6 from Test 1, outcrops of salt crystals were not found.

Test Procedure 3 – Sample 12

Within the samples for Test 3, Mšene showed definite accumulation of salt on the surface when analysed with SEM-EDS. Similarly, to the observation from Test 1 and 2, a crust had developed on the surface, however it appears to be less salt concentrated than in Test 1 and 2. In the middle row, right image of Figure 25, even visually the salt crusts seems to cover less of the stone's grains. However, the HyperMap point analysis did confirm that it was pure sodium sulfate on top of the sandy particles.

Recalling from section 4.2.1 General Observations, the Božanov and Opuka specimen did not show any significant alterations due to mass loss. However, Božanov developed a crust on the sides exposed to evaporation and Opuka samples had white dusty particles on it's surfaces up to the height reached by the wet front during the wetting phase. These surface deposits were believed to be salt, yet under the scanning electron microscope, no salt was observed in with the MultiPoint or HyperMap elemental mapping (see top row Figure 25). A few structures in the Božanov sample, such as the one shown Figure 25, were investigated, but EDS analysis showed them to be binder.

When the first sample of Opuka was analysed (OP12 evap.) no salt was seen. Due to the easily visible, dusty white particles on Opuka at the height of the absorption water front, the presence of salt in this portion of the specimen seemed likely. A second sample of Opuka, explicitly from this region with the deposits, was analysed to determine if the surface deposit was salt. An elemental mapping point, shown in Figure 25, found 5.3% Na2O and 15.2% SO3. If a second sample from the Božanov samples was also taken from an area with the surface crust, the presence of salt may have been identified with the EDS elemental mapping.

As previously discussed, it is difficult to observe the salts in Opuka. However, from the observations of Božanov and Mšene, the fact that Test procedure 3 called for rewetting with water three out of four cycles, it's believed that some of the salt content was washed away in the re-wetting cycles.

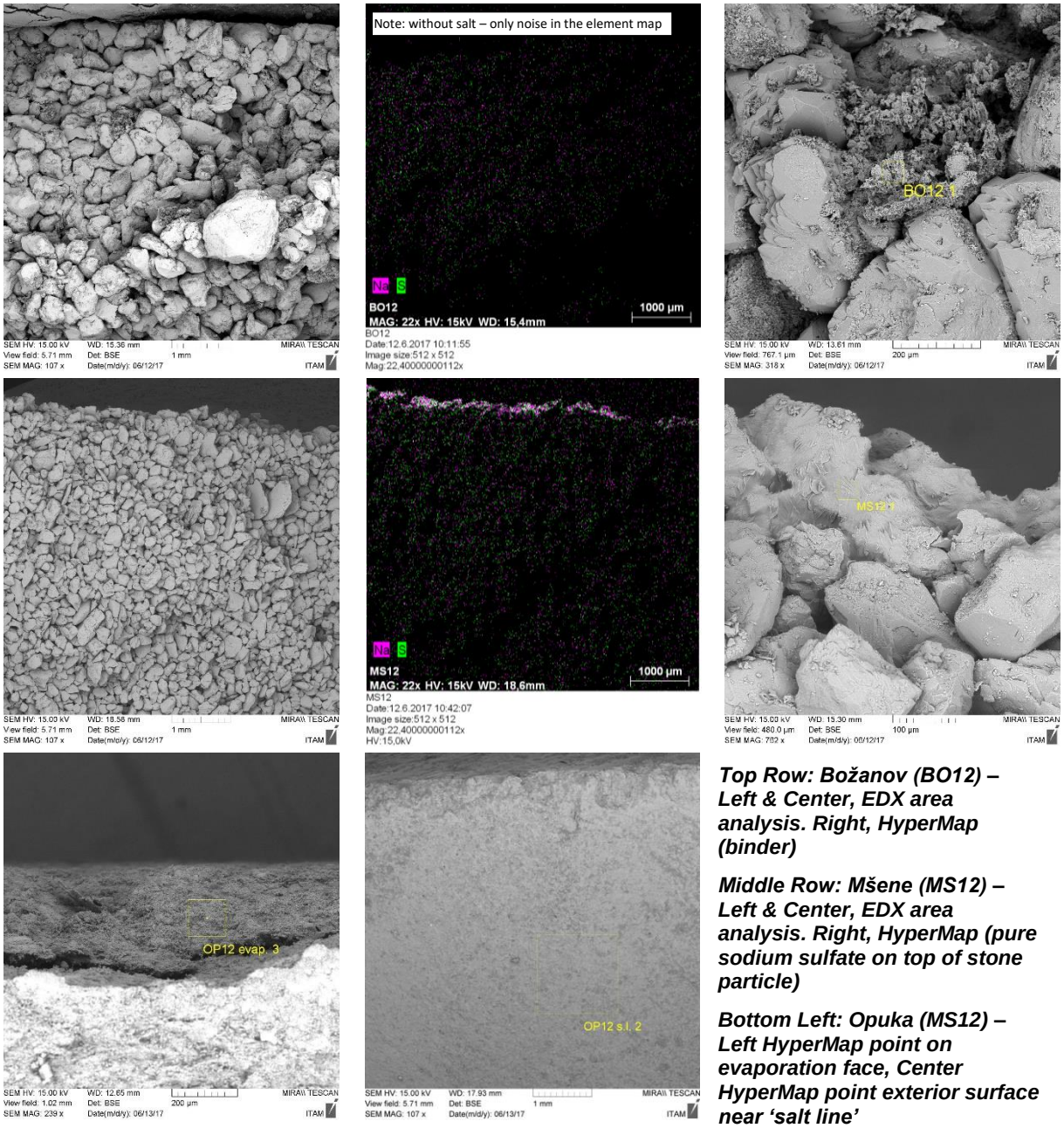

Top Row: Božanov (BO12) – Left & Center, EDX area analysis. Right, HyperMap (binder)

Middle Row: Mšene (MS12) – Left & Center, EDX area analysis. Right, HyperMap (pure sodium sulfate on top of stone particle)

Bottom Left: Opuka (MS12) – Left HyperMap point on evaporation face, Center HyperMap point exterior surface near 'salt line'

Figure 25: SEM Analysis of samples from Test 3

Test Procedure 4 – Samples 15

In all three of the stone types, a surface crust was observed for specimens subjected to Test 4 (Figure 26). For Božanov, a distinct surface crust was not seen in Test 1 (Figure 24), however a notable amount of salt in a very uniform distribution was noted. It's suggested that the lower drying temperature in Test 4 slowed down the drying process, allowing more time for the mechanics of capillary transport to draw more salt to the surface of specimens of Božanov in Test 4 versus Test 1.

A surface crust was seen on Mšene samples for Test 1-3, so it's observation in the sample from Test 4 was anticipated. The close-up analysis of the salt crust showed a layer of salt crystals (Hyper Map point

2 & 3) covering particles of the stone (HyperMap point 1). Specifically, the 3rd HyperMap point suggests that at least portions of the sodium sulfate crystal are in a hydrated phase (hepta- or deca-hydrate) as the salt crystal was sensitive to the electron beam of the SEM when elemental mapping was conducted (black dot caused by beam). It's difficult to say if the sodium sulfate was never completely dehydrated during the final drying phase, or if thenardite crystals rehydrated due to exposure to ambient humidity and temperature for the purpose of the SEM analysis.

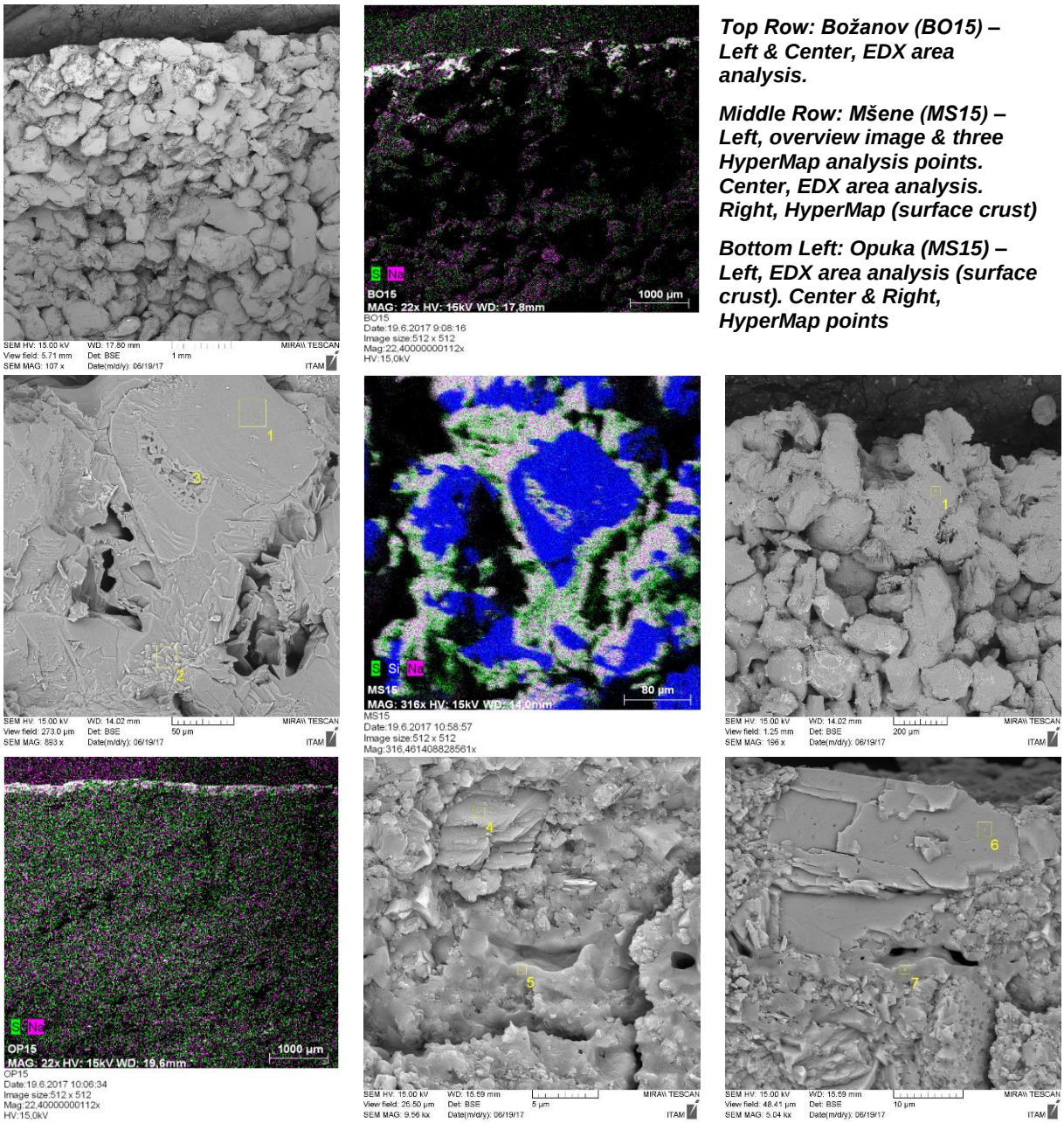

Top Row: Božanov (BO15) – Left & Center, EDX area analysis.

Middle Row: Mšene (MS15) – Left, overview image & three HyperMap analysis points. Center, EDX area analysis. Right, HyperMap (surface crust)

Bottom Left: Opuka (MS15) – Left, EDX area analysis (surface crust). Center & Right, HyperMap points

Figure 26: SEM Analysis of samples from Test 4

Since no surface crust was observed in Test 1 and in general a lack of salt was seen in any of the Opuka samples, the clear surface crust exhibited on this sample was somewhat unexpected (bottom row Figure

26). Close up analysis of the area (center and right image) showed that points 5 and 7 are sodium sulfate crystals on top of the fabric of the stone. Once again, this accumulation of salt near the surface compared to the other Tests is attributed to the lower drying temperature, and therefore slower drying speed allowing the salt solution to accumulate close to the surface.

Test Procedure 5 – Samples 18

Observations from the other analysis techniques have found little to no damage induced in the samples used in test procedure 5. The results of the SEM-EDS hold true to this pattern, with no observation of salt in the fabric of the Božanov and Opuka samples. Some crystals of salt were found in the sample of Mšene, however when the elemental area analysis was conducted, even Mšene showed no signs of a surface crust. The use of 7wt.%, partial immersion, and rewetting with water in Test 5 prevented pore filling with sodium sulfate, supporting the lack of decay seen in these samples. More cycles would be required to achieve damage form this testing procedure.

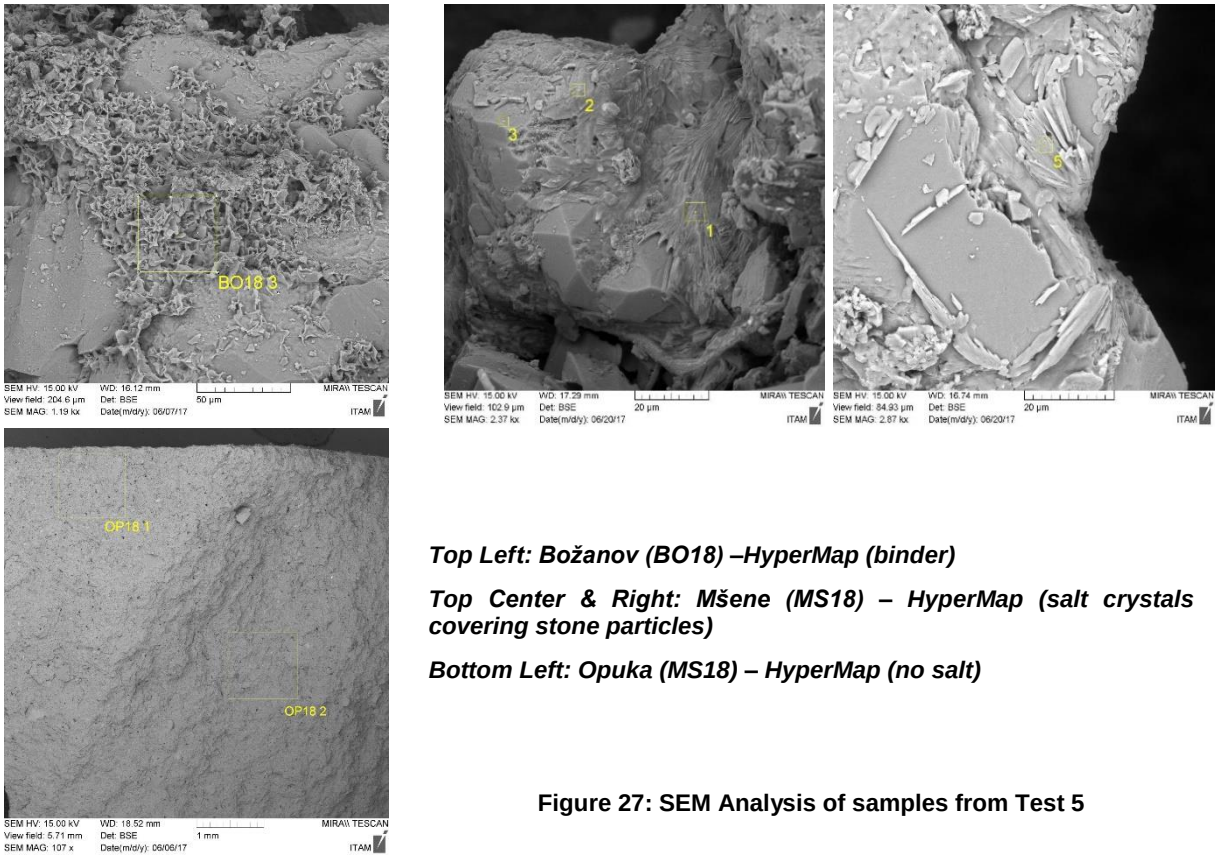

Top Left: Božanov (BO18) –HyperMap (binder)

Top Center & Right: Mšene (MS18) – HyperMap (salt crystals covering stone particles)

Bottom Left: Opuka (MS18) – HyperMap (no salt)

Figure 27: SEM Analysis of samples from Test 5

5. DISCUSSION AND RECOMMENDATIONS

The objective of this thesis research was developed in line with the objectives of the RILEM Technical Committee 271-ASC working to develop an '*Accelerated laboratory test for the assessment of the durability of materials with respect to salt crystallization'*. The scope of this committee is significantly broader and more in depth then the present research. However, the thesis objective was aimed at considering the impact of modifying certain parameters of the existing EN12370 standard for the determination of resistance to salt crystallization, in order to find a more effective and realistic use of sodium sulfate for accelerated salt crystallization aging tests. Additionally, several different assessment techniques (SEM-EDS, UPV, salt distribution, mass loss, mass variation and visual observations) were used to investigate the effectiveness and reliability of each testing technique in determining the durability of the material. Details of the data and observation from each assessment method have been discussed in the preceding sections. Following is a synthesis of this information with the aim of discussing properties of the stones that are related to their durability; comparison and discussion of the effectiveness and representativeness of the different testing factors used; and, discussing which techniques were most effective in assessing the damage.

5.1 Durability characteristics and prediction

In summary, Mšene samples exhibited the most materials loss, followed by Opuka and Božanov. Opuka has the smallest pore size making it susceptible to salt decay, however from the greater deterioration of Mšene it is evident that pore size can not be the only factor [5]. Other factors, such as open porosity and mechanical strength, have an impact as it affects the quantity of water, and therefore salt, a material can absorb. Furthermore, pore size will impact the capillary transport mechanisms within a material. Therefore, although Opuka's small pore size makes it more susceptible to damage from crystallization pressure, the larger pore size of Mšene and Božanov mean the materials can become rapidly saturated with water (or salt solution) and dry at a rapid rate. In real conditions, this allows for more wet/dry cycling to occur leading to increased damage.

Within this research, the three stone types all had monomodal PSD. With the aim of developing a standard test for many types of material, the influence of more heterogenous pore networks should also be considered. Moreover, the combination of different materials with different PSDs is an important aspect in the overall behaviour of the constructive element. As has been found in other research studies [20] and confirmed in this work, the durability of a porous material does not depend on a single factor. To make accurate predictions, the degree that each factor, such as pore size, open porosity, pore shape, crack density, homogeneity of the pore network, and mechanical strength, has to be analysed in terms of its individual importance and the overall importance of all the properties combined. Further, when assessing the durability of materials already in use in heritage constructions, it is important to note that past weathering can increase the porosity of a stone and modify the general fabric of a material, which in turn affects its durability [5]. Differences in a stone fresh from a quarry and those that have experienced years of weathering, possibly developed crusts and/or experienced chemical changes, can

be significant [3]. Therefore, if durability results from a laboratory test on a new specimen are to be used to inform decisions about an existing structure, the results must be calibrated to account for the existing weathered condition of the in-situ material.

5.2 Testing Procedure

Consideration of the testing parameters such as salt solution concentration, partial or complete immersion, rewetting with water, and drying temperature are important in making a testing procedure that is effective and realistic. One aim of the RILEM committee includes defining aggressiveness classes to help manage the many interrelated variables of salt aging to help establish a quantifiable ranking of durability, and ensure materials are being tested for conditions that they will be required to withstand. The finding of the research with respect to changing different parameters and how they might play into the definition of aggressiveness classes is discussed following.

Comparing the level of decay between the five different tests, the use of 14wt.% mirabilite solution in comparison to 7wt.% seems to have the greatest effect of all the factors varied. Specimens in the test where 14wt.% solution was used (Test 1, 3 and 4) demonstrated faster and more decay. This is a positive effect with respect to accelerating the damage, however it does not reflect reality as in-situ salt content is usually around 1-2% [3]. As discussed previously, a higher salt content can also increase the required drying time of the specimen due to the hygroscopic nature of salt. It would be more realistic to increase the number of cycles to accelerate the testing process than to increase the salt solution concentration. In many of the studies investigating the durability of materials to salt crystallization, a higher number of cycles is usually required to achieve damage using the EN12370. Goudie [38], observed that salt weathering appears to be a cumulative effect. As discussed previously, it is the number of wet/dry activations that is the most important for sodium sulfate to induce damage [3]. In conclusion, for realistically accelerating salt aging test it is recommended to increase the number of wet/dry cycles rather than increasing the salt solution concentration, because very high salt concentrations are not representative of real conditions.

The use of partial or complete immersion appeared to have the next greatest impact on the results of the test. Although the discrepancy in results was greatly impacted by the porous characteristic of the stones. For Mšene, which has the largest absorption coefficient and open porosity values, the difference in mass evolution was small between partial and complete immersion (when comparing between tests with the same concentration of salt) compared to the results for Opuka and Božanov. The debate comes back to acceleration of the test versus realistic testing parameter. In real buildings, sources of moisture and contamination fluctuate with the environment, therefore exposure may not be long enough to fully saturate low absorbing materials, which can contribute to heterogenous decay. Future testing procedures could be developed to be adapted to different environmental aggressiveness classes as is recommended by the RILEM committee. In this case, the average duration moisture will be present in the environment to wet the material can be considered in combination with the absorptive properties of

the materials in order to decide if the material is likely to be completely or only partially saturated in the field.

For test procedures 3 and 5 where contamination was done once every four cycles and then re-wetting was done with distilled water in between, very little to no damage was observed for samples of Božanov and Opuka. For Mšene sandstone, the samples in Test 3 which uses 14wt.% salt solution demonstrated notable decay. However, those in Test 5 with 7wt.% did not. Researchers Matthieu et al. [19] considered the effect of simply remobilization of salts and concluded that it was not sufficient to cause damage; additional salt need to be provided by the solution. Nevertheless, from the results of this experiment, it seems that the high salt content (14wt.%) in Test 3 combined with the large absorption capacity and absorption rate of Mšene is sufficient to ensure the presence of enough salt to cause supersaturation when re-wetted with water. However, the lower concentration in Test 5 prevent the level of salt required to reach supersaturation. With respect to Test 3 for Božanov and Opuka, the absorption capacity and absorption rate inhibit salt uptake compared to Mšene. Furthermore, the increases mechanical strength means greater level of supersaturation are required to develop sufficient stress to induce damage. As the level of salts in an environment can change with location, thereby affecting if more salt would be introduced to a material each time wetting occurs. For environments that are less contaminated with salt, the aging test could be modified to introduce more realistic concentrations of salt (1-2% for sodium sulfate [3]). The other parameters in the test should also be adapted to be more realistic (e.g.: lower drying temperature) and therefore draw the salt towards the surface, allowing supersaturation to be achieved in the same manner observed in real conditions.

The variation in drying temperature between 105˚C and 60˚C did not show any drastic impact on the deterioration of samples with all other factors constant. Some evidence from the SEM and visual observations would suggest that the lower drying temperature did cause more salt to be drawn to the exterior of the stone, thus creating a higher area of salt concentration and slightly more damage. Nevertheless, more testing with additional cycles should be done to study and more accurately quantify the difference in salt distribution caused by the different drying temperatures. As discussed in the State of the Art the effect of temperature on the supersaturation and crystallization of mirabilite is significant (see section 2.2.1). Observations from an experiment where wetting was carried out at temperature of 3, 10, 20, and 25˚C saw damage after the first cycle at the cooler temperatures, where more cycles were required to induce damage in the warmer tests [7]. The range and average temperature of the climate for which a material will be used should be taken into consideration when designing an aging test. The definition of the aggressiveness classes could consider a ‘standard temperature range’ and in addition to having a class that considers aggressive conditions due to elevated salt content, one class could be tailored to cold climates.

In an effort to move towards a more realistic salt crystallization aging test, the influence of several parameters on the aging process of natural stones was assessed. Three types of stone with varying porous structure and mechanical strengths were used to help assess the impact of the of each

parameter. Some variables, such as a lower drying temperature only had detectable effects on one stone type. Other factors, such as salt solution concentration, showed significant impact in all stones. Hence the importance of using materials with a varying of intrinsic characteristic when designing an accelerated aging test.

5.3 Analysis Tests

Of the different analysis tests carried out each has its pros and cons. General observations and tracking the mass evolution is a simple technique, not requiring a lot of equipment or time. A basic representation of the materials decay can be given by the normalized mass evolution, however insight into the process of the material's decay is limited. Collecting lost material from specimens as they deteriorate can help in separating the amount of salt uptake versus, mass loss encompassed in the overall mass evolution. But this requires a lot of time to carefully collect, wash, dry and weigh the debris.

Ultrasonic Pulse Velocity (UPV) is a simple technique in addition to being able to use the technology on-site to asses existing structure. However, based on the inconclusive results of this experiment further in-depth study would be required to correlate the ultrasonic velocity with internal deterioration in the specimens. Other studies have used this technique for assessment of salt weathering, and previously a lot of research has gone into correlating physical properties of materials with UPV. Therefore, it is considered that it could still be a useful assessment tool once reliable relationships between the ultrasonic velocity and material decay can be established. Other researchers have even proposed that it could be an effective predictor of durability [5].

The distribution of salt in a material is due to a combination of environmental parameters and the physical properties of the test specimen. Therefore, understanding where in a sample salt crystallizes helps to evaluate and assess damage. Moreover, assessing the salt distribution by conductivity is a very time-consuming process. The use of the Hygroscopic Moisture Content test for determining salt distribution should also be considered as it is an inexpensive and less work intensive technique [1].

SEM is a useful tool for investigating the distribution in the pores and the morphology of sodium sulfate within the stones. It is a more time consuming and expensive technique of evaluation, and only small samples of a specimen can be observed. Furthermore, although it provides key information about how and where salt crystallizes in the samples, it is not useful for objectively quantifying the degree of damage in a specimen.

Another analysis technique that could be considered to assess the level of alteration in the specimens is MIP. This testing takes time but is not work intensive, however it would require too many samples to be an ongoing assessment technique. It would be used to assess the sound and final weathered states. If samples are too deteriorated, this testing may not be possible, but it can provide useful information about changes to the porous network

5.4 Future Work

To continue the work of developing a new effective, realistic, and quantifiable accelerated salt crystallization aging test, the following tests and conditions could be considered:

- Additional testing based on EN12370, but with lower and more variations in drying temperature to evaluate what temperature provides a balance between realistic simulation of building conditions with a reliable and effective accelerated salt weathering test;
- Additional testing based on EN12370 with smaller concentrations of sodium sulfate to establish how many cycles and which different concentrations are required to induce damage in materials with diverse physical and mechanical properties;
- Conduct salt aging test with one or more surfaces of the specimen sealed to consider the impact of limited contamination and evaporation surfaces;
- Consider effect of different salts (e.g. NaCl, Na2CO3, MgSO4, NaNO3, Ca2SO4) and the combination of salts in accelerated salt crystallization tests;
- Test combining building materials (e.g. mortar and masonry units) to assess the positive and negative effects the different materials have on each other through out a salt weathering test;
- Assess aging evolution with Ultrasonic Pulse Velocity with the aim of establishing a reliable correlation between UPV, damage, and durability. Ensure changes in the samples size and uneven contact surface of the damaged specimen are considered;
- Define levels of aggressiveness (with respect to e.g. temperature, relative humidity, salt type and concentration) for a future salt crystallization test to assess durability.

REFERENCES

[1] T. C. D. Goncalves Dias, "Salt crystallization in plaster or render walls," Universidade Tecnica de Lisboa, Lisbon, 2007.

[2] U.S. Geological Survey, "Sodium Sulfate Statistics and Information," U.S Department of the Interior, 17 December 2016. [Online]. Available: https://minerals.usgs.gov/minerals/pubs/commodity/sodium_sulfate/. [Accessed 31 06 2017].

[3] B. Lubelli, R. van Hees and T. Nijland, "Salt crystallization damage: how realistic are existing ageing tests?," in *3rd International Conference on Salt Weathering of Buildings and Stone Sculptures*, Brussels, 2014.

[4] M. Angeli, J.-P. Bigas, D. Benavente, B. Menendez, R. Hebert and C. David, "Salt crystallization in pore: quantification and estimation of damge," *Environmental Geology,* vol. 52, no. 2, p. 187*195, 2007.

[5] M. Angeli, J.-P. Bigas, D. Benavente, B. Menendez, R. Hebert and C. David, "Modification of the porous network by salt crytallization in experimentally weathered sedimentary stones," *Materials and Structure,* vol. 41, no. 6, pp. 1091-1108, 2008.

[6] J. Desarnaud, F. Bertrand and N. Shahidzadeh-Bonn, "Impact of the kinetics of salt crysllallization on stone damage during rewetting/drying and humidity cycling," *Journal of Applied Mechanics,* vol. 80, pp. 1-7, 2013.

[7] R. J. Flatt, F. Caruso, A. M. A. Sanchez and G. W. Scherer, "Chemomechanics of salt damage in stone," *Nature Communications,* p. 5:4823, 2014.

[8] M. Steiger and A. Sönke, "Crystallization of sodium sulfate phases in porous materials: The phase diagram Na2SO4-H2O and the generation of stress," *Geovhi,ica et Cosmochimica Acta,* vol. 72, no. 17, pp. 4291-4306, 2008.

[9] G. W. Scherer, "Stress from crystallization of salt," *Cement and Concrete Research,* vol. 34, no. 9, pp. 1613-1624, 2004.

[10] R. Prikryl, "Durability assessment of natural stone," *Quarterly Journal of Engineering Geology and Hydrogeology,* vol. 46, pp. 377-390, 2013.

[11] T. Wiiffels and B. Lubelli, "Development of a new accelerated salt crystallization test," *Heron,* vol. 51, no. 1, pp. 63-79, 2006.

[12] CEN, "EN 12370 Natural stone test methods - Determination of resistance to salt crystallisation," Netherlands Standard Insitute, 1999.

[13] R. van Hees and H. Brocken, "Damage development to treated brick masonry in a long-term salt crystallisation test," *Construction and Building Materials,* vol. 18, pp. 331-338, 2004.

[14] H. Derluyn, T. A. Saidov, R. M. Espinosa-Marzal, L. Pel and G. W. Scherer, "Sodium sulfate heptahydrate I: The growth of single crystals," *Journal of Crystal Growth,* vol. 329, no. 1, pp. 44-51, 2011.

[15] N. Tsui, R. J. Flatt and G. W. Scherer, "Crystallization damage by sodium sulfate," *Journal of Cultural Heritage ,* vol. 4, no. 2, pp. 109-115, 2003.

[16] ICCROM, Laboratory handbook - Porosity, Vols. 1-2, C. McDowall and C. Rockwell, Eds., Rome: International Centre for the Study of the Preservation and Restoration of Cultural Property, 1999.

[17] E. Wendler and A. Charola, "Water and its Interaction with Porous Inorganic Building Materials," in *5th International Conference on Water Repellent Treatment of Building Materials* , Brussels, 2008.

[18] RILEM, "RILEM 25-PEM, II.5: Evaporation curve," *Mater. Constr.,* vol. 75, no. 13, pp. 205-207, 1980.

[19] M. Angeli, J.-P. Bigas, D. Benavente, B. Menendez, R. Hebert and C. David, "Influence of capillary properties and evaporation on salt weathering of sedimentary rocks," *Heritage Weathering and Conservation,* vol. 1, pp. 253-259, 2006.

[20] S. Yu and C. T. Oguchi, "Role of pore size distribution in salt uptake, damage, and predicting salt susceptibility of eight types of Japanese building stones," *Engineering Geology,* vol. 115, no. 3-4, pp. 226-236, 2009.

[21] J. Teutonico, A laboratory manual for architectural conservators, Rome: ICCROM, 1988.

[22] A. Ahmad, M. Pamplona and S. Simon, "Ultrasonic testing for the investigation and characterization of stone - a non-destructive and transportabel tool," *Studies in Conservation,* vol. 54, pp. 43-53, 2009.

[23] R. Přikryl, Z. Weishauptová, M. Novotná, J. Přikrylová and A. Šťastná, "Physical and mechanical properties of the repaired sandstone ashlars in the facing masonry of the Charles Bridge in Prague (Czech Republic) and an analytical study for the causes of its rapid decay," *Environmental Earth Sciences,* vol. 63, no. 7-8, pp. 1623-1639, 2010.

[24] J. Ďoubal, "The restoration of the Stone Fountain in Kutná Hora: An assessment of the contemporary intervention within the context of repairs throughout history," *Studies in Conservation,* p. 1–13, 2016.

[25] ITAM, "Final Report: The Conditions and Requirements for Compatible Care for Porous Inorganic Materials (NAKI18)," ITAM, Prague, 2015.

[26] E. Vejmelková, M. Keppert, P. Reiterman and R. Černý, "Mechanical, hygric and thermal properties of building stones," *Structural Studies, Repairs and Maintenance of Heritage Architecture,* vol. 131, pp. 357-367, 2013.

[27] J. Ďoubal, "The restoration of the Stone Fountain in Kunta Hora: An assessment of the contemporary intervention within the context of repairs throughout history," *Studies in Conservation,* 2016.

[28] Z. Pavlík, P. Michálek, M. Pavlíková, I. Kopecká, I. Maxová and R. Černý, "Water and salt transport and storage properties of Mšené sandstone," *Construction and Building Materials,* vol. 22, no. 8, pp. 1736-1748, 2007.

[29] R. Přikryl, J. Přikrylová, M. Racek, Z. Weishauptová and K. Kreislová, "Decay mechanism of indoor porous opuka stone: a case study from the main alter located in the St.Vitus Catherdral, Prague (Czech Republic)," *Environmental Earth Sciences,* no. 7, pp. 1-15, 2017.

[30] J. Konta, "Stone of a Gothic Pieta discovered in Bern: Comparison with Cretaceous marly chert from Prague," *Applied Clay Science,* vol. 7, no. 5, pp. 357-366, 1993.

[31] V. Schutznerova-Havelkova, "The use of snady marlstone in the medieval architecture of Prague," 1978.

[32] R. Přikryl, J. Svobodová, Z. Weishauptová and T. Lokajíček, "Experimental weathering of marlstone from Přední Kopanina (Czech Republic) - historical building stone of Prague," *Building Environment,* vol. 38, pp. 1163-1171, 2003.

[33] J. Rouquerol, D. Avnir, C. Fairbridge, D. Everett, J. Haynes, N. Pernicone, J. Ramsay, K. Sing and K. Unger, "Recommendations for the charachterization of o=porous soilids," *Pure & Applied Chemistry,* vol. 66, no. 8, pp. 1739-1758, 1994.

[34] B. D. Zdravkov, J. J. Čermák, M. Šefara and J. Janků, "Pore classification in the characterization of porous materials: A perspective," *Central European Journal of Chemistry,* vol. 5, no. 2, pp. 385-395, 2007.

[35] T. J. Mays, "A new classification of pore sizes," *Studies in Surface Science and Catalysis,* pp. 57-62, 2007.

[36] M. Prat and N. Sghaier, "Effect of efflorescence formation on drying kinetics of porous media," *Transport in Porous Media,* vol. 80, pp. 441-451, 2009.

[37] M. Angeli, "Multiscale study of stone decay by salt crystallization in porous networks, PhD. Thesis," Université de Cergy Pontoise, Cergy, 2007.

[38] A. S. Goudie, "Laboratory simulation of 'The Wick Effect' in salt weathering of rock," *Earth Surface Processes and Landforms,* vol. 11, no. 3, pp. 275-285, 1986.

[39] R. Rossi-Manaresi and A. Tucci, "Pore structure and the disruptive or cementing effect of salt crystallization in various types of stone," *Studies in Conservation,* vol. 36, no. 1, pp. 53-58, 1991.

[40] C. Cardell, D. Benavente and J. Rodrigues-Gordillo, "Weathering of limestone building material by mixed sulfate solutions. Characterization of stone microstructure, reaction products and decay forms," *Materials characterization,* vol. 59, pp. 1371-1385, 2008.

APPENDIX A: SODIUM SULFATE DECAHYDRATE CONDUCTIVITY CURVE

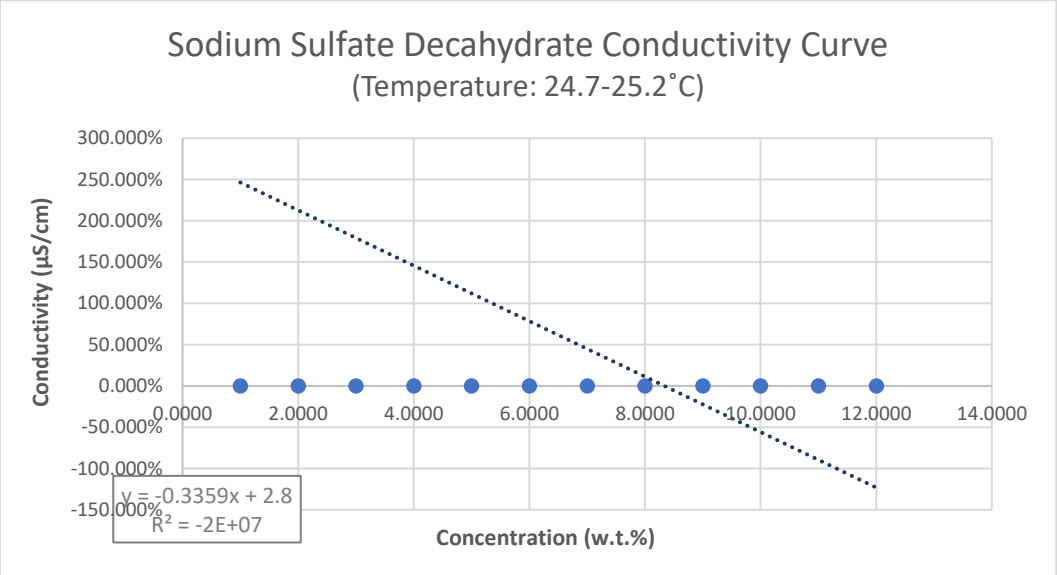

Graph 15: Sodium Sulfate Decahydrate Conductivity Curve (0.0-0.1w.t.%, 24.7-25.2˚C)

Along with sodium sulfate and other ions from the dissolved stones, temperature also has an impact on conductivity. Therefore, while developing the conductivity curve and measuring each sample's conductivity, it was ensured that the temperature of the solutions were similar, although some discrepancy were unavoidable. The conductivity curve was developed with solutions ranging in temperature from 24.7-25.2˚C, while all the stone solutions were measured at temperatures ranging from 24.0-24.7˚C.